We thank the reviewers for the very detailed comments that have helped improve the manuscript. Following the reviewers' comments, we have made several changes to the manuscript.

1. Several clarifications were added in the introduction and discussion.
2. Several technical imprecisions were corrected.
3. More information on the retrieval convergence and degrees of freedom of the system were added in Section 4 to better address the information content in the retrieval of the Cf parameter.
4. For this purpose, Fig. 7 c and d were changed and now show the averaging kernel matrix and one example of convergence.
5. The comparison between retrievals with and without scattering is now shown using the same algorithm and radiative transfer (instead of MWRRET). This is shown in the new Fig. 8 (c,d).
6. The retrieved drop size distributions are now shown in the new Fig. 8(a,b)
7. Two new tables were added to show the characteristics of the clouds analyzed in this work. These also show optimal conditions for the application of the retrieval.
8. A discussion on the conditions to apply the retrievals is added in section 5
9. A discussion of the limitations of the retrieval is added in Section 4.
10. A few references were added.

Responses to RC1 (ref#2)

We thank the reviewer for very detailed comments on the manuscript. Responding to them has substantially improved the manuscript. The reviewer's comments are italicized and responses are in red.

The paper by Cadeddu presents a new technique to retrieve column integrated values of drizzle water below and above cloud base as well as cloud water above the cloud base.
The technique is well presented, but is only applied only to a small data set. However, the paper fails to provide necessary information to evaluate if the technique can be applied, for example, only to geometrical thin clouds or only to warm clouds. I would be good to know the range of, e.g. cloud optical and geometrical thickness or cloud top temperature of the clouds that can be considered as potential targets for the technique.

To address this concern, we added more discussion on this in section 5 at lines 417-428. Rather than specific atmospheric conditions under which the technique can be used, below we report specific criteria under which the technique can be applied,

1) The radar and ceilometer are not attenuated by precipitation and are able to adequately detect the cloud base and cloud top.
2) The radiometer measurements are not affected by precipitation on the lens.
3) The drizzle droplet diameter is large enough to be detected by the 90 GHz channel (in other words the technique will not work in very light drizzle).
4) The cloud can be considered close to be adiabatic so that the cloud and in-cloud drizzle water content can be modeled with sufficient confidence.

Given these criteria the applicability of the technique can be different for ground-based and airborne instrumentation, and for a combination of the two. For example, if we had a radiometer looking down instead of looking up the criterion #2 would be satisfied for a broader range of precipitating clouds than what was presented in this work, as long as the other criteria are met. The attenuation at Ka-band wavelength is significant during heavy precipitation, making it not possible to retrieve below-cloud cloud drizzle properties. The adiabaticity of marine stratocumulus clouds changes on shorter (less than minute) timescales, with sub-adiabatic downdrafts and super-adiabatic updrafts (Stevens et al. 1998, Wood, 2012). However, the clouds are nominally adiabatic on minute or longer timescales, suitable for application of this technique. We have also added in Tables 3-5 the estimated optical depths for the clouds in this work (assuming a cloud drop effective radius of 10 μm) and the geometrical thickness from the radar-estimated cloud top and the ceilometer-estimated cloud base. We think that the value reported are optimal for the application of this technique.

Stevens, B., W.R. Cotton, G. Feingold, and C. Moeng, 1998: Large-Eddy Simulations of Strongly Precipitating, Shallow, Stratocumulus-Topped Boundary Layers. J. Atmos. Sci., 55, 3616–3638, https://doi.org/10.1175/1520-0469(1998)055<3616:LESOSP>2.0.CO;2

The authors should also state if the technique only works for single cloud layers or how the observed LWP would be distributed over multi-layered clouds.

We used the technique for single layer clouds. In the open cell dataset examined for this work there were several occurrences of heavy precipitating stratocumulus clouds with non-precipitating shallow cumulus clouds in the layers below. These cases were usually heavy precipitating and therefore the passive retrieval was not applied. Theoretically, the technique could be applied to multi-layer clouds, however, as the reviewer mentioned here, a realistic representation of the cloud boundaries and LWP may be needed. This was added in section 5 lines 423-425.

Can the method could also be applied to Arctic clouds?

The falling ice/snow below a mixed phase Arctic clouds can potentially scatter the microwave radiation at 90 GHz emitted by the liquid water within the cloud. However, that will depend significantly on the shape and size of the ice crystals. This is outside the scope of this work and hence at this stage we can't recommend this methodology for Arctic clouds.

It would be very helpful if the authors would provide a brief review on cloud-droplet size distributions and drizzle size distributions. What are typical values in the literature for warm stratocumulus clouds? The calculated cloud droplet diameters shown in Figure 5 seem quite large and the drizzle diameters rather small.

Thank you for raising this issue. A comprehensive survey of cloud drop size distributions have been carried out by Miles et al. (2000) with estimates from multiple field campaigns reported in various articles e.g. DYCOMS-II Stevens et al. (2003 BAMS), VOCALS Zheng et al. (2011 ACP), Bretherton et al. (2010 ACP), EPEACE (Russell et al. 2013) and CSET (Albrecht et al. 2019). A comprehensive review of stratocumulus clouds is also provided in Wood et. al. (2011) and Wood (2012).
Due to the large variability of in-cloud and precipitation microphysical properties (diameter and number) both vertically and horizontally due to turbulence and aerosol-cloud interactions, many of these estimates are for bulk properties such as rain rates, LWC and LWP. Tables 3 and 5 now added to this work provide information of typical properties for these clouds.

Miles, N.L., Verlinde, J. Clothiaux, E. E.: Cloud Droplet Size Distributions in Low-Level Stratiform Clouds, *J. Atmos, Sci.*, 57, 295--311, 2000.

R. Wood, C. S. Bretherton, D. Leon, A. D. Clarke, P. Zuidema, G. Allen, and H. Coe: An aircraft case study of the spatial transition from closed to open mesoscale cellular convection over the Southeast Pacific, *Atmos. Chem. Phys.*, 11, 2341–2370, doi:10.5194/acp-11-2341-2011, 2011

Wood, R.: Stratocumulus clouds, *Mon. Weather Rev.*, 140, 2373--2423, 2012.

Minor comments:

Line 87: calculations are based . . . for non-spherical and oriented particles. How are spherical droplets (cloud/drizzle) handled in the model?

The single scattering properties of spherical droplets such as cloud, drizzle, or rain are calculated with the Mie theory. For the radiative transfer solver RT4 it doesn't matter if the particles are spherical or non-spherical. It simply gets the 4 by 4 scattering and extinction matrix and the emission vector as input. These have to be calculated or provided by appropriate methods.

Line 89: what do you understand under ice crystal habit?

By ice crystal habits we mean the shape, density, size, mass-size relation, and so on. All that which differentiates frozen particles in terms of radiative properties.

Line 212: What drizzle size was observed? Please add a figure of the observed DSD in cloud and below cloud for the different cases and add in Table 2 and 3 the mean cloud and drizzle (in and below cloud) diameter, CTT, and optical and geometrical thickness.

We added in Fig. 8, left panels (new) the distribution of the retrieved drizzle diameter below cloud base and what was retrieved immediately above cloud base with the radar only. Because the number of columns was too large to keep in one table, we added tables 3 and 5 with the shaft-averaged drizzle diameter found below and above cloud base, cloud top temperature, optical and geometrical thickness. Throughout the paper the cloud droplet diameter is assumed constant with a value of 10 micron. This value is also used in the calculations of the optical depth.

Figure 1: add the observed precipitation at ground

We added panel 1d with the precipitation at the ground observed by the video-disdrometer. Because of the large range of precipitation values the vertical axis is shown in log scale.

Figure 2/line 109: Drizzle modal diameter is not shown in the Figure 2. Please change. Also, change the colour scale, maybe use a log scale. Now it is only shown to 500 µm. It should extend to the 800 µm (largest diameter stated in the text).

Accepted. Thank you for this suggestion.

Figure 5b, black line is missing.

For this case which was at the very onset of the drizzle event the black line was entirely under the blue line. We state this in the caption now.

Other comments:
Figure 5, yellow is not a good choice of colour. The contrast is very poor.

Changed to green. Thanks.

Figure 7, The colour in the legend and the plotted data seem not to be the same.

Figure 7 was changed, and the colors were changed to be the same. Thanks.

Responses to RC2 (ref #1)

General comments

This manuscript presents a new technique for obtaining cloud and drizzle liquid water path by combining multi-channel microwave radiometer, Doppler cloud radar and ceilometer measurements. The new technique is applied to observations of precipitating stratocumulus clouds and evaluated qualitatively by comparison with Doppler cloud radar spectra.
The technique shows great promise and will aid the community investigating the properties of stratocumulus by providing a new piece of information, although the full potential is not explored deeply in this initial study. This manuscript is almost ready for publication, with a few technical aspects to correct.

Thank you for the review and the kind words. We hope to perform a more extensive study in the near future on the impact of these results on aerosol-precipitation interactions. Our responses to your comments are below in red.

Technical comments

Line 18: Replace 'exists' with 'exist'. Accepted.

Line 22: Suggest opening with 'Marine stratocumulus clouds have a significant impact on the Earth's radiation balance as they reflect a greater amount of solar radiation back to space compared to the ocean surface, and emit a similar amount of longwave radiation as the surface.' Accepted.

Line 26: Replace 'Feingold and A. McComiskey 2016' with 'Feingold and McComiskey 2016'. Thanks for catching that. It has been replaced.

Line 31: Move comma from after 'properties' to after 'instrumentation'. Accepted.

Line 32: Do you mean moments here, or would it be more realistic to state 'the shape of the drop size distribution'? Otherwise you should explain what you mean by moments in this context.

We have replaced the sentence to read. "From the point of view of ground-based instrumentation, the study of microphysical and macro-physical cloud properties involves combining data from multiple instruments to retrieve parameters of the hydrometeor drop size distribution (DSD). For example, the radar reflectivity is proportional to the sixth moment of the DSD and was used to retrieve liquid water content that is the third moment of DSD by Frisch et al. (2002)."
Thanks.

Lines 35-36: This statement needs some qualification. Review papers discussing LWP estimation from multi-channel microwave radiometers usually state that care must be taken in the presence of precipitation, and that LWP estimates are not reliable in strong precipitation.

We agree with the reviewer and clarified this statement in lines 53-57. Added 2 references on the topic (Wall et al., 2017 and Bosisio et al., 2013).

Line 58: Replace 'since summer of 2015' with 'since the summer of 2015'. Done-Thank you
Line 61: Suggest stating 'reflectivity-weighted Doppler spectrum'. Done

Line 61: Replace 'Collocated to' with 'Collocated with'. Done

Line 63, 75, 92 and elsewhere: *Replace 'backscatter' with 'attenuated backscatter'.* Done for all instances. Thanks for pointing this important difference.

Line 71: The correct reference for 'auto-calibration of cloud lidar' is O'Connor et al. (2004) not (2005). Done

Line 103: Lidar ratio for cloud droplets at 905 nm is about 19 sr, and is even lower for larger drizzle droplets. Changed

Line 104: The ceilometer attenuated backscatter peaks at cloud base due to the large return from the small but much more numerous cloud droplets, relative to drizzle droplets. Changed

Line 106: Do you mean here, 'the average modal diameter of the full drop size distribution including drizzle drops and cloud droplets'? How reasonable is this assumption considering that these are two distinct hydrometeor populations, normally giving rise to a skewed distribution if they overlap?

Yes, and we agree with the reviewer that this is not the optimal solution. This assumption was very much debated among the authors and we resorted to this option because there is really no sensible way of separating the two distributions. This assumption was only used in the passive retrieval as a way forward to constrain the drizzle size in the cloud. It may require a separate study to understand how optimal this assumption is. In a recent study Glienke et al. (2017) pointed out that the cloud and drizzle distributions are almost in a continuum in marine stratocumuli. However, as they are measured by separate in situ probes, and modelled through different processes, the cloud and drizzle DSD are often assumed to be separate.

Glienke, S., A. Kostinski, J. Fugal, R. A. Shaw, S. Borrmann, and J. Stith (2017), Cloud droplets to drizzle: Contribution of transition drops to microphysical and optical properties of marine stratocumulus clouds, *Geophys. Res. Lett.*, 44, 8002–8010, doi:10.1002/ 2017GL074430.

Line 161: Small drizzle drops may not display a negative Doppler velocity if they are falling into a strong updraft. It is true to state that drizzle drops have a significant terminal fall velocity, but the observed Doppler velocity is the sum of the fall velocity and the air motion.

Thank you for raising this point and we agree with the reviewer that drizzle drops falling in updraft will not fall and rather go upwards, and the radar reported mean Doppler velocity is the sum of the droplet fall velocity and the air motion.

However, we resorted to converting the Doppler velocity to diameter as i) the focus of this study is on (relatively) larger drizzle drops with diameters greater than 100 micrometers that scatter radiation from the cloud and have fall velocity of 0.3 m/s spanning six Nyquist velocity bins ii) the Doppler spectra are averaged on minute timescales in an attempt to minimize the contribution from turbulence, and iii) for the cases analyzed here we didn't encounter a Doppler spectra entirely on the positive velocity.

The sentence has been rephrased as follows: "The methodology is based on the fact that the Doppler spectra of a non-precipitating cloud is centered on zero mean velocity due to their movement with turbulence, while that containing falling drizzle drops is negatively skewed due to their fall velocity. Hence, the presence of drizzle drops in a cloud introduces a negative skewness in the cloud Doppler spectra."

Line 167: Suggest using the term 'drizzle shafts' here and elsewhere in the manuscript. Done.

Line 176: Suggest rephrasing to '.. are as negatively skewed as the Doppler spectra at cloud base'. Accepted.

Lines 177-178: The terminal fall velocity of cloud droplets is very small, and their observed Doppler velocity distribution is a result of turbulence. Added.

Line 185: Not quite true. For Rayleigh scattering, reflectivity is proportional to mass- squared, but the larger drizzle drops are in the Mie scattering regime.

The reviewer is correct that for large drizzle drops that are under Mie scattering regime, the radar reflectivity is not proportional to mass-squared. Our forward model calculations show the Mie-to-Rayleigh backscatter ratio to be 1 for diameters below 400 micrometers, increasing to 1.2 for diameters of 1000 micrometers at Ka-band wavelength (Ghate and Cadeddu, 2019 JGR).

For the drizzle drops analyzed here, we estimate a maximum error of 20% due to this assumption. Further, even under the Mie scattering regime the area under the curve of the Doppler spectra will be still proportional to the mass of the condensate, albeit with a different proportionality than square. We have rephrased the sentence as follows:

"The areas under the final cloud and drizzle spectra (indicated by the red and yellow stripes respectively) are proportional to the total mass of cloud and drizzle liquid water responsible for the radar signal under the Rayleigh scattering regime with some modifications during Mie scattering regime."

Line 264: Do you mean in-cloud DWP here? Yes, it was intended above cloud base, we changed it with "in-cloud".

Figure 1: 'together with cloud boundaries from KAZR (cloud top) and ceilometer (cloud base)' 'ceilometer attenuated backscatter coefficient'. Changed

Figure 4: In (a), does cloud LWP include in-cloud drizzle (DWP) or cloud droplet LWP only?
It only includes cloud droplets.

Figure 5: 'Downward motion'. It is not clear how the x-axis is derived.
We used the relationship between size and velocity in Gossard et al., 1990: r=av+b with a=1.4E-4 and b=1E-5. This is now stated in the caption.

Figure 10: The solid line represents the mean of the total LWP measured in each flux divergence bin? How about the bars? The figure caption should be clear.

Thank you, that was forgotten. The caption was rephrased as follows: The black circles connected by a solid line represent the total LWP binned by flux divergence and the vertical bars represent the standard deviation of the data in each bin.

Responses to RC3 (ref#3)

We thank the reviewer for a detailed review. Please find below our responses to your comments. Your comments are in black and our responses are in red.

1. *One of the main findings of this paper concerns the importance of considering scattering effects in microwave retrievals. However, I have a few concerns with the ways these results are obtained.*
A first way to evaluate the scattering effect is through comparisons between the retrievals and their associated a priori values from a neural network algorithm that doesn't consider scattering. I am not very convinced with the impact on C_f, which seems to stay close to its a priori value, but a reduction of LWPt is indeed clearly observed. Is the optimal estimation framework used for this study based on a Levenberg-Marquardt scheme, i.e. is a departure from the a priori value actually showing a reduction of the cost function (rather than being possible iteration noise in a Gauss-Newton approach)? Please comment on this, and for future study I'd suggest using more quantitative metrics like the cost function, information content or degrees of freedom to reach such conclusions.

Yes, the convergence is monitored through a reduction of the cost function and through a convergence criterion as explained in the 2017 paper (C2017) eq 4. Because the problem is fairly well defined the convergence is very quick. The aspects mentioned by the reviewer are very relevant and they are at the very heart of the problem. The main reason why they were not addressed in more details in this work is because they were analyzed in detail in C2017 and here we wanted to focus more on the application of the retrieval rather than the retrieval itself, and also not to repeat previous analysis. Nonetheless, given the importance of the topic we have expanded section 4 and included more references to the results from the 2017 paper.

As it can be seen in Fig. 6 and 8 and Table I of C2017 the C_f showed a small improvement with respect to the a priori. The degrees of freedom were also analyzed in Fig. 7 where it was found that the DOF of the system for C_f varied depending on the physical constraints on the system. In this work a few changes were made, in particular only 3 quantities are retrieved and the drizzle DSD is provided. The a priori information for C_f is also better constrained because is derived with the help of the active retrieval. Although it is true that the change in C_f is not large, it is also possible that the a priori information provided is in within the limits of what can be achieved with this technique. The a-posteriori uncertainty of this parameter shown in Fig. 7a (this work) does show a reduction.

We have now included in Fig. 7 c and d more details on the retrieval. Fig. 7c shows the third element of the averaging kernel matrix A(3,3) defined in Eq. 5 of C2017 in relation to the average drizzle diameter. Fig. 7d shows one example of convergence. In this case (as in the majority of the cases that were able to converge) convergence is achieved at the 3rd iteration. In Fig. 7d for example the C_f parameter is quickly adjusted from 0.73 to 0.59. On the right axis of Fig. 7d we now show the cost function is shown. A(3,3) represents the varying contribution of the measurements to Cf that depends partially on the amount of scattering that the model attributes to the scene. The discrete values are due to the truncation of the DFS values to the first decimal digit.

Another way the importance of scattering is quantified is by comparing the retrievals of the new technique to those of MWRRET2, a similar retrieval algorithm. Considering the importance of these results, more details of the similarities / differences between the retrieval algorithms should be given in section 2.1. But why not simply turn scattering off (forcing the single-scattering albedo to 0) in your current retrieval algorithm, instead of using a different retrieval algorithm? That would avoid being impacted by retrieval technique differences and be much more convincing.

We thank the reviewer for this comment. This is actually something that was debated during the writing of the manuscript. The rationale for showing the comparison with MWRRET was that, because users are going to utilize MWRRET, they may be interested in knowing how much scattering is affecting that retrieval. However, we also see the point of the reviewer here and agree that using the same radiative transfer code and methodology has its merits as it eliminates possible differences and biases due to the different retrievals. Therefore, we have rerun the retrievals for the open cell cases setting the drizzle to zero. The results are now shown in Fig. 8 c,d.

2. *The impact of shafts on retrievals is discussed, first in the algorithm description and then in the result discussions. But it is still not clear to me, especially in the discussions surrounding Tables 2 and 3, what part of the conclusions concern impacts from retrieval limitations or from actual microphysics differences during shafts. Please clarify the exact (expected) impact of shafts on retrievals, so that the readers can more clearly understand your results.*

Although the retrievals were performed on a time resolution of 1 minute, the results were analyzed statistically, in terms of shaft averages. This because instantaneous properties of drizzle shafts may be dominated by turbulent processes, however average properties are important to understand physical processes that affect the larger scales.
It is our opinion that the different characteristics between open cell and close cell systems evidenced in Tables 2-5 (2-3 in the previous version) are actual micro- and macro-physical differences and not artifacts of the retrievals. Tables 3 and 5 report results from the active part of the retrieval which is a fairly well-established technique. As for the passive retrievals (Tables 2 and 4) there are two main limitations that affect the results: the first limitation concerns the lack of sensitivity of the microwave to drop sizes smaller than ~ 100 μm. This limitation affects both open and closed call cases, however given that the frequency of occurrence of small drops is higher in closed cell systems it will probably lead to a larger underestimation of in-cloud DWP in these systems. The second limitation concerns the inability of the microwave to retrieve during the time of more intense precipitation. This will only affect the open cell cases and will result in an underestimation of the average shaft CWP and DWP. The quantification of the impact will likely require an LES model. We added these comments in section 4, lines 341-349.

Ground-based Observations of Cloud and Drizzle Liquid Water Path in Stratocumulus Clouds

Maria P. Cadeddu [1], Virendra P. Ghate[1], and Mario Mech[2]
[1]Environmental Sciences Division, Argonne National Laboratory, Argonne, IL, 60439, USA
[2]University of Cologne, Cologne, 50969, Germany
Correspondence to: Maria P. Cadeddu (mcadeddu@anl.gov)

Abstract. The partition of cloud and drizzle water path in precipitating clouds plays a key role in determining the cloud lifetime and its evolution. A technique to quantify cloud and drizzle water path by combining measurements from a three-channel microwave radiometer (23.8, 30, and 90 GHz) with those from a vertically pointing Doppler cloud radar and a ceilometer is presented. The technique is showcased using one-day of observations to derive precipitable water vapor, liquid water path, cloud water path, drizzle water path below the cloud base, and drizzle water path above the cloud base in precipitating stratocumulus clouds. The resulting cloud and drizzle water path within the cloud are in good qualitative agreement with the information extracted from the radar Doppler spectra. The technique is then applied to ten days each of precipitating closed and open cellular marine stratocumuli. In the closed cell systems only ~20% of the available drizzle in the cloud falls below the cloud base, compared to ~40% in the open cell systems. In closed cell systems precipitation is associated with radiative cooling at the cloud top < -100 W/m^2 and liquid water path > 200 g/m^2. However, drizzle in the cloud begins to exist at weak radiative cooling and liquid water path > ~150 g/m^2. Our results collectively demonstrate that neglecting scattering effects for frequencies at and above 90 GHz leads to overestimation of the total liquid water path of about 10-15%, while their inclusion paves the path for retrieving drizzle properties within the cloud.

1 Introduction

Marine stratocumulus clouds have significant impact on the Earth's radiation balance as they reflect a greater amount of solar radiation back to space compared to the ocean surface and emit a similar amount of longwave radiation as the surface. The processes affecting their highly organized spatial structure, and their spatial and temporal variability are a topic of active research (Wood et al. 2015). Precipitation is hypothesized to play an important role in the transition between different mesoscale organizations of boundary layer clouds (Feingold and McComiskey 2016; Wang and Feingold, 2009). Similarly, precipitation, together with entrainment, impact the cloud microphysical properties that determine the cloud radiative effects (Wood, 2012; Yamaguchi et al., 2017). Hence, characterizing the properties of drizzling stratocumulus clouds through observations and high-resolution models for furthering our understanding of the precipitation processes has been a focus of several previous studies (e.g. Ahlgrimm and Forbes, 2014; Zheng et al. 2017). From the point of view of ground-based instrumentation, the study of microphysical and macro-physical cloud properties involves combining data from multiple instruments to retrieve parameters of the hydrometeor drop size distribution (DSD). For example, the radar reflectivity is proportional to the sixth moment of the DSD and was used to retrieve liquid water content that is the third moment of DSD by Frisch et al. (2002). For this purpose, new algorithms are developed that can extract key cloud and drizzle properties such as liquid water content and drop effective radius from a combination of active (e.g. radar, lidar), and passive (broadband or narrowband radiometers) sensors (e.g. Frisch et al., 1995; Fielding et al., 2014). Microwave radiometers have been extensively used in the past in such retrieval techniques to obtain the total column (i.e. cloud and drizzle) liquid water path of a precipitating cloud. By adding a 90 GHz or 183 GHz channel to the traditional 23 and 30 GHz channels, the uncertainty in the retrieved LWP (and column water vapor) can been reduced significantly (Löhnert and Crewell, 2003). Ground-based retrievals in precipitating or even drizzling conditions are however still an area of active research. Granted that heavy precipitation does affect the measurements by altering the dielectric properties of the surface over which water deposits, the degree to which light precipitation affects the retrieval outcome is still unclear (Wall et al., 2017, Bosisio et al., 2013). Recent theoretical studies (Cadeddu et al., 2017) have shown that drizzle-sized hydrometeors (larger than 90 microns in diameter) significantly scatter the radiation at 90 GHz and could also be used to derive separate estimates of integrated drizzle water and cloud water.

In this work we propose a technique to retrieve column integrated values of i) drizzle water path below the cloud base (DWP_{bc}), ii) drizzle water path above the cloud base (DWP_{ac}), and iii) cloud water above the cloud base (CWP) by combining the data from vertically pointing cloud radar, lidar, and a microwave radiometer. The technique is applied to 20 days of data collected at the Atmospheric Radiation Measurement (ARM) Eastern North Atlantic (ENA) site during light to moderate precipitating stratocumulus cloud conditions. In **section 2** an overview of the methodology is provided followed by application to one day of data. I**n Section 3** the results are qualitatively assessed by comparison with radar-observed Doppler spectra. The entire dataset of 20 days is examined in **section 4** through averages of in-cloud and below-cloud-base drizzle properties for the precipitating shafts, and the relation between LWP, turbulence, and drizzle production is shown. The results are summarized and briefly discussed in **Section 5**.

2 Methodology

In Sect. 2.1 an overview of the instrumentation and the radiative transfer models is provided. The use of active sensors to derive microphysical properties of drizzle below cloud base is well established and is used in the first part of the algorithm, the active module, described in Sect. 2.2. In the second part of the algorithm, named the passive module, resides the novel approach of using scattering properties of drizzle drops to separate cloud and drizzle water path within the cloud. The passive module is described in Sect. 2.3.

2.1 Instrumentation and Radiative Transfer Models

The ARM ENA site has been operational since the summer of 2015 and is located at the northern tip of the northernmost island Graciosa (39° N, 28° W, 15 m) in the Azores. The site has many instruments, and here we describe those used in this work. A vertically pointing Ka-band Doppler radar named Ka-band ARM Zenith Radar (KAZR) continuously records the raw reflectivity-weighted Doppler spectrum and its first three moments at 2 s temporal and 20 m range resolution. Collocated with the KAZR is a laser ceilometer (lidar) that operates at 905 nm wavelength and reports the first three optical cloud base heights and the raw attenuated backscatter at 15 s temporal and 30 m range resolution. A three-channel microwave radiometer is also present at the site that records the calibrated brightness temperatures at 23.8, 30 and 90 GHz frequencies at 10 s temporal resolution. Balloon borne radiosondes are launched at the site every 12 hours at 00 and 12 UTC. Due to the sparseness of the radiosonde launches, the radiosonde data is interpolated with that from the ECMWF model to deduce profiles of temperature, pressure, humidity and winds at a uniform 1-minute temporal and 50 m vertical resolution. The visible imagery and cloud top temperature reported by the Spinning Enhanced Visible Satellite Imager (SEVIRI) onboard geostationary Meteosat satellite were used to confirm the presence of similar cloud conditions around the site as those observed at the site.

The ceilometer attenuated backscatter was filtered for noise using the technique proposed by Kotthaus et al. (2016), and was calibrated following O'Connor et al., (2005) using data collected on 7 March 2016. More details about the ceilometer calibration are mentioned in the Appendix of Ghate and Cadeddu (2019), referred to as GC19 from hereon. The KAZR was calibrated by comparing its reflectivity with that from the Ka-band Scanning ARM Cloud Radar that was calibrated using a corner reflector. The KAZR calibration hence is good within 1 dB. The KAZR and ceilometer data were combined to produce estimates of the first three moments of Doppler spectra and of ceilometer attenuated backscatter on a uniform 1 min temporal and 50 m range resolution following Clothiaux et al. (2000). These were further used to calculate cloud boundaries. Microwave radiometer data are collected by a 3-channel radiometer (23.8, 30, 90 GHz). The radiometer is calibrated using tip curves (Han and Westwater, 2000) resulting in a calibrated brightness temperature uncertainty of about 0.3 K in the K-band and 1 K in the W-band. The resulting uncertainty in the derived products is about 0.4 kg/m^2 for PWV and 15 g/m^2 for LWP. Precipitable water vapor and liquid water path derived using a neural network algorithm (Cadeddu et al., 2009) are provided in the data file. These retrievals are derived with an absorption-only radiative transfer model, MonoRTM (Clough et al., 2005) and are used as a priori information in the algorithm described in this work.

We use the *Passive and Active Microwave TRAnsfer (PAMTRA) Package* (Mech et al., 2018) available at https://github.com/igmk/pamtra, a scattering microwave radiative transfer model that simulates active and passive measurements in plane parallel geometry between 1 and 800 GHz. The calculations are based on the fully polarized model of Evans and Stephens (1995) for non-spherical and oriented particles. The model simulates passive measurements in upward and downward geometry at a given height and allows the choice between different assumptions and models in the calculations of surface emissivity, ice crystal habit, size distribution, and calculation of scattering properties. The Rapid Radiative Transfer Model (RRTM) (Iacono et al., 2000) was used to calculate the radiative fluxes and heating rates. We refer the reader to GC19 regarding the details of the setup and inputs of RRTM.

An example of the noise filtered profiles of KAZR reported reflectivity, ceilometer reported attenuated backscatter and the concurrent retrievals of LWP from MWRRET2 (Turner, 2007) in non-scattering approximation are shown in Fig. 1 (a–c). Moderate to heavily precipitating stratocumulus clouds were observed throughout the day, with most of the precipitation evaporating before reaching the surface. Precipitation measurements at the surface from the video-disdrometer are shown in Fig. 1 (d).

2.2 The active module

The active module of the retrieval technique is similar to that proposed by O'Connor et al. (2005) and applied to the ARM data by GC19 with some subtle differences. Drizzle below the cloud base is assumed to have a three-parameter gamma drop size distribution. The ceilometer attenuated backscatter, radar reflectivity, mean Doppler velocity and width of the Doppler spectra were used in an iterative manner to retrieve the three parameters of the gamma distribution. Details of the radar-lidar microphysical retrievals of drizzle properties below the cloud base are given in GC19 together with an extensive discussion of the range of validity of the algorithm. The lidar signal attenuates at the cloud base as the lidar ratio (extinction to backscatter) of cloud drops is 50-60 Sr compared to 19 Sr or lower of drizzle drops at the 905 nm wavelength. Hence, the ceilometer attenuated backscatter peaks at the cloud base due to the presence of smaller but more numerous cloud drops in addition to the drizzle drops. The returns at the cloud base from pixels containing both cloud and drizzle drops were neglected by GC19. In this work we assume the DSD of these cloud and drizzle mix to have a lognormal shape with a width of 0.38 and retrieve the modal diameter and number concentration. These serve as an a priori information in the retrieval framework.

The retrieved modal diameter and rain rate for the case shown in Fig. 1 are shown in Fig. 2 a and b. During this day, the drizzle modal diameter was between 100 and 800 μm and rain rate was around 2.5 mm/day with brief peaks greater than 10 mm/day. Precipitation shafts were identified using the criteria explained in G19 and shown as black solid lines in Fig. 2 a. In this specific case 24 drizzle shafts were identified with measurable precipitation detected at the surface for some of the drizzle shafts. Although this does not constitute a problem for the active instrumentation it does affect the passive module because excessive water deposition on the radiometer can affect the data. At the cloud base the average modal diameter of the mixed drizzle-cloud DSD was 77.8 μm.

2.3 The passive module

The output from the active (radar-lidar) module is used as input to the microwave radiative transfer model. The theoretical basis for the retrieval is provided in Cadeddu et al. (2017). In this operational implementation only three quantities are retrieved: PWV, total liquid water path (LWPt), and C_f, the ratio of cloud to total water path. The radiative transfer code, PAMTRA, used in the passive module requires information on the cloud and drizzle DSD, specifically liquid water content, the shape parameter, and effective diameter. Because the microwave measurements are insensitive to the gamma parameter of the DSD this last is set to zero in the passive module denoting exponential distribution. The below cloud drizzle water content (DWC_{bc}), below cloud drizzle water path (DWP_{bc}) and the average drizzle effective radius below cloud base calculated from the active module are provided to the radiative transfer model. These properties of drizzle below are kept intact during the entire iterative process within the passive module. Figure 3 shows a flow chart of the active and passive modules with the quantities provided as input, the intermediate outputs, and the final output. Additional details of the passive module are provided in Table 1.

Because *in-cloud* properties are not easily derived and the active module is only valid at and below cloud base, several assumptions had to be made about the *in-cloud* DSD parameters. The drizzle water content *above cloud base* (DWC_{ac}) is assumed constant with value equal to the drizzle water content at the cloud base (Wood, 2005), and the cloud water content (CWC) is assumed to follow an adiabatic profile (Zuidema et al., 2005). The initial adiabatic profile is determined by subtracting the initial drizzle water path (Table 1, row 6) from the initial total LWP (LWP_t in Table 1, row 2) and distributing the resulting cloud water path adiabatically between cloud base and top. These estimates of CWP and the first guess LWP_t are used to provide the first guess estimate of C_f as shown in the flowchart (Table 1, row 9). At each iteration the drizzle water path above cloud base (DWP_{ac}) and CWP are adjusted based on LWP_t and C_f to ensure consistency with the drizzle below cloud base by scaling the liquid water content accordingly. Once the retrieval converges the diagonal elements of the covariance matrix can provide information on the reduction of the uncertainty of the three retrieved parameters.

The retrieval of the C_f parameter depends on how much the scattering information affects the measurement and is therefore dependent on the drop size distribution. It is expected that the retrieval will be more effective during precipitation characterized by drops larger than 100 μm in diameter. The advantage of having larger drops is however offset by the fact that they usually reach the surface which impacts the convergence because of water deposition on the radiometer window. This limitation of the ground-based instrument is evident in Fig. 2c where the total LWP from this work is shown during precipitating shafts. On November 21, 2016 the retrieval converged in 367 out of the 484 minutes identified in the drizzle shafts. Using the proposed technique from aircraft or satellite will enable to study a wider range of precipitating conditions and to take better advantage of the scattering information. In fact, based on a similar principle, Jacob et al., (2019) applied a neural network retrieval to microwave measurements collected from aircraft to separate cloud from drizzle water path over the Atlantic Ocean.

Total, cloud, and drizzle water path during the first 4 hours of 21 November 2016 (minute 1-240) are shown in Fig. 4 a and b. Although the below-cloud drizzle is well defined in the active retrieval process, the information that can be gained from the microwave retrieval on the partition of cloud and drizzle depends on how much information is available from the measurements. The CWP constitutes the largest portion of the total LWP, and the resulting total drizzle water path (in cloud and below cloud) is in this case about twice the precipitating drizzle. In the next section the in-cloud partition between drizzle and cloud water path is closely examined next to the radar Doppler spectra during 21 November 2016.

3 Comparison with the Radar Doppler Spectra

Due to lack of coincident other retrievals of cloud and drizzle water within the cloud layer, here we qualitatively evaluate them by separating the cloud and drizzle contributions in the Doppler spectra. Possible ways and the challenges of quantitively evaluating these retrievals are discussed in the last section.

3.1 Radar spectra processing

Doppler spectra from cloud radars have been previously used to gain insight into the onset and evolution of drizzle in clouds (Kollias et al., 2011a, 2011b; Luke and Kollias, 2013; Acquistapace et al., 2019). The methodology is based on the fact that the Doppler spectra of a non-precipitating cloud is centred on zero mean velocity due to their movement with turbulence,

while that containing falling drizzle drops is negatively skewed due to their fall velocity. Hence, the presence of drizzle drops in a cloud introduces a negative skewness in the cloud Doppler spectra. In this section, cloud Doppler spectra are analyzed with the intent of separating the cloud and drizzle components to qualitatively evaluate their co-variability.
In the following analysis the Doppler spectra were averaged for one minute to reduce the effect of turbulence and they were denoised using the technique of Hildebrand and Sekhon, (1974). Doppler spectra for six drizzle shafts that lasted for more than 20 min on 21 November 2016 and for which the microwave retrieval converged at least 75% of the times are analyzed. Figure 5 shows examples of Doppler spectra from the drizzle shaft that developed between 04:22 and 05:50 UTC (minutes 262-350 in Fig. 1 and 2). The shift in the location of the peak towards negative velocity near the cloud base (Fig. 5a) indicates the presence of drizzle drops that dominate the radar signal. Gates near the cloud top on the other hand have peaks centered around the zero velocity, indicating the presence of cloud drops. It is also noticeable in Fig. 5a the increase in the power of the signal as drizzle drops become the dominant contribution to the radar reflectivity. To separate the drizzle from the cloud contribution in the power spectra the assumption was made that the signal originating near the cloud top is *mostly* generated by cloud droplets. This assumption holds true in weak and moderate drizzling conditions however fails in heavily precipitating clouds when the Doppler spectra at the cloud top are as negatively skewed as the Doppler spectra at cloud base. The spectra for layers near the cloud top were vertically averaged and fitted to a Gaussian distribution. The terminal fall velocity of cloud droplets is very small, and their observed Doppler velocity distribution is a result of turbulence. The standard deviation of the near-cloud-top Gaussian distribution was taken as representative of the velocity spread of the cloud droplet distribution through the cloud. Cloud-only spectra near the cloud top at 04:29, 04:35, and 04:56 UTC are shown in blue in Fig. 5 (b, c, d). Note that the vertical velocity was converted into drop diameter using the relation between fall velocity and diameter from Frisch et al., (1995) and Gossard et al., (1990). To isolate the cloud component, the right shoulder of the curve is fitted to a Gaussian distribution with standard deviation given by the cloud-only distribution (red curve). When this estimated cloud component is subtracted from the cloud-averaged spectra, the resulting distribution (shown in green) is considered representative of the drizzle-only signal. The areas under the final cloud and drizzle spectra (indicated by the red and green stripes respectively) are proportional to the total mass of cloud and drizzle water responsible for the radar signal under the Rayleigh scattering regime with some modifications during Mie scattering regime. Although the analysis is qualitative, it can be seen that the procedure captures the evolution of the drizzle from its initial stage to a stage where the drizzle component becomes more prominent in the cloud.

3.2 Radar and radiometer

The areas under the red and green curves shown in Fig. 5 (b, c, d) are shown in Fig. 6 a, b for two entire drizzle shafts (04:22– 05:50 UTC and 21:41–22:24 UTC). The radiometer-retrieved CWP and DWP_{ac} (black and red lines in Fig. 6 c, d) follow a similar time evolution. The missing points are times when the passive retrieval failed to converge. It should be noted that, as explained is Sect. 2, the drizzle water path below cloud base derived by the active module is used, together with an initial estimate of total LWP, to estimate the a priori partition between cloud and drizzle water path. During the retrieval process the algorithm adjusts the PWV, total, and cloud water path (C_f) to achieve convergence based on the microwave radiometer measurements. During this process both the cloud water and in-cloud drizzle water path are adjusted. Therefore, a correlation between the radar information and the radiometer retrieval is expected. Fig. 6 shows that the retrieval process conserves the information provided by the radar and, while adjusting the total liquid water path to be consistent with the scattering properties of the hydrometeors, it provides final estimates of CWP that are consistent with the radar in-cloud information and with the radar-provided retrievals below cloud base. In the two examples below, the radar and radiometer both show that the CWP component is dominant through the drizzle shaft and the DWP_{ac} increases to reach a maximum after about 10 minutes. The retrieved total LWP in these two drizzle shafts shows that during the times of maximum drizzle development the DWP_{ac} reaches at the most 10-15% of the CWP. The quantification of the DWP in relation to the total LWP and CWP is examined in the next section.

4 Analysis of results and potential applications

In this section cloud and drizzle water path derived on 10 days each of open cellular and closed cellular stratocumulus cloud conditions observed at the ENA site are analyzed and discussed. The purpose of this section is to evaluate whether the results are consistent with the current state of knowledge of stratocumulus clouds and to provide ideas for possible applications of these results to the study of turbulence, drizzle production, drizzle formation, and cloud-aerosol interaction.

Before proceeding with the details of the drizzle and cloud water path partition some general features of the retrieval applied to the 10 open cell cases are shown. The open cell cases are selected as they contain larger drizzle drops leading to greater scattering of the microwave signal, however similar conclusions can be drawn for the closed-cell data. Fig. 7a shows the reduction in the uncertainty of C_f (ratio of CWP to total LWP) after the retrieval converges. The retrieval has a larger impact in cases where the drizzle diameter below cloud base is larger than 200 μm (Fig. 7a). A C_f value of unity corresponds to no drizzle drops present within the cloud layer, and a value of zero corresponds to absence of any cloud sized drops in the cloud layer. The final retrieved C_f varies between 0.5 and 1 (no drizzle) and is shown in Fig. 7b vs the a priori C_f for clouds with LWP greater than 150 g/m^2. Collectively Figure 7a and 7b demonstrate the reduction in the uncertainty of C_f due to the retrieval process. After the retrieval converges the averaging kernel matrix **A** from eq. 5 in Cadeddu et al. (2017) is related to the independent pieces of information (or degrees of freedom of the system) provided by the measurements. The third diagonal element A(3,3) of the matrix, shown in Fig. 7c, represents the varying contribution of the measurements to the retrieval of C_f. Finally, an example of the convergence process for one retrieval point is shown in Fig. 7d. The retrieval starts with a first guess and adjusts the three retrieved parameters until the convergence criteria specified in eq. 4 of Cadeddu et al. (2017) is satisfied. The process minimizes a cost function that is monitored at each iteration to ensure proper convergence. The convergence process is very quick and is usually completed after two or three iterations as shown in Fig. 7d.

As mentioned in Sect. 2.1, the a priori total liquid water path (LWP_t) used to start the convergence process is derived with a neural network algorithm (Cadeddu et al., 2009) with no-scattering assumptions. The present retrieval generally reduces the LWP_t with respect to the a priori and the reduction is more pronounced for cases affected by scattering to a larger extent.

However, for a better understanding of the overall impact of the scattering effect on the total LWP, the same retrievals were performed without scattering, assuming that the LWP is distributed entirely in the cloud layer. Figure 8 (a, b) shows distributions of the retrieved drizzle mode diameter below (red) and above (black) cloud base for the closed cell (a) and open cell (b) cases. In Fig. 8 (c, d) the effect of the drizzle diameter on the retrieved LWP is examined by looking at the relative differences between the LWP retrieved with scattering (LWP_{sc}) and without scattering (LWP_{nosc}). The relative differences in Fig. 8d are computed as $100*(LWP_{nosc}-LWP_{sc})/LWP_{nosc}$. *Accounting for scattering effects reduces the total liquid water path by about 8-20% depending on the drizzle diameter*. This result provides a quantification of the uncertainty that can be expected from neglecting scattering effects during precipitating conditions. For thicker clouds with $LWP_t > 500$ g/m^2, neglecting the scattering effects of drizzle drops when using the 90 GHz channel can potentially lead to an overestimation of LWP by ~100 g/m^2, far higher than the accuracy needed for characterizing the aerosol-cloud interactions.

A summary of the average cloud and drizzle characteristics in the drizzle shafts for each open cell and closed cell days analyzed are reported in Tables 2 to 5. The cloud optical thickness was broadly estimated assuming a constant cloud drop effective radius of 10 μm using the relation: $\tau=9CWP/5\rho_w r_e$ (Painemal and Zuidema, 2011). From Tables 2 and 4 it is evident that in closed cellular stratocumuli 70-80% of the total drizzle is found in the cloud and less than 30% of the total drizzle in a shaft falls below the cloud base. While in open cellular stratocumuli, on average 30-50% of the total drizzle is precipitating with most of it falling below cloud base. The modal diameter of drizzle within the cloud is almost twice in open cellular stratocumuli than that compared to closed cellular stratocumuli. The ratio of below-cloud drizzle drop diameter to in-cloud drizzle drop diameter is ~2 for open cellular stratocumuli and ~3 for closed cellular stratocumuli, confirming drizzle being ubiquitous in these clouds with only some of it falling below the cloud base in both mesoscale organizations. There are two main limitations that affect the results shown in tables 2 and 4: First the lack of sensitivity of the microwave channels to drop sizes smaller than ~ 100 μm, which increases the uncertainty in the retrieved DWP. This limitation affects both open and closed call cases, however as the number of small drops is higher in closed cellular stratocumuli than in open cellular stratocumuli, a larger underestimation of DWP in the cloud can be expected in closed cellular stratocumuli. The second limitation concerns the inability of the microwave radiometer to measure brightness temperatures during intense precipitation due to water deposition on the radome. This will only affect the open cell cases and will result in an underestimation of the average drizzle shaft DWP in the cloud. As expected, the total LWP is larger in the open cell cases compared to the closed cell, even accounting for the retrieval underestimation due lack of convergence during times with the highest precipitation.

The co-variability of the total (in-cloud + below-cloud) DWP and the CWP is explored in Fig. 9. Shaft averaged values of DWP and CWP are binned in bins centered at 50, 150, 250 and 350 g/m^2 with a width of 100 g/m^2. The total (in-cloud + below-cloud) drizzle water path in the shaft is a small fraction (generally less than 30%) of the CWP and increases with the cloud water path. This behavior is consistent with the findings of Lebsock et al. (2011). The DWP increase is more pronounced in the open cell (shown in black) than in the closed cell (shown in red) systems, and for a similar amount of CWP greater amount of drizzle is present in the open cellular drizzle shafts. This is further examined in Fig. 10 where the cumulative distribution of the ratio of precipitating-to-total drizzle water path in the shaft is shown segregated by the average drizzle diameter at the cloud base. The figure shows that the fraction of drizzle water path leaving the cloud is higher in shafts that, on average, have larger droplets. Virtually all closed cell cases (blue line) have a drizzle diameter less than 200 microns (GC19) and for 90% of them the fraction of drizzle water path below the cloud is less than 0.2. In the same range of drizzle diameter open cell drizzle shafts (black line) show higher precipitation fraction with 90% of the shafts having below-cloud to total ratio of 0.4 or less. Finally, in 80% of the drizzle shafts with larger average drop sizes (red line) the ratio of below-cloud to total drizzle water path is 0.6 or less.

The partition of cloud and drizzle water path is also important when studying the relation between turbulence and precipitation. As an example, Fig. 11 shows the total (a), below-cloud-base (b), and above-cloud-base (c) drizzle water binned by the radiative flux divergence at the cloud top and by total LWP for all 1-min averaged closed cell cases. The figure illustrates the relation between drizzle, LWP, and turbulence. Clouds with strong divergence (less than -100 W/m^2) have high probability of developing drizzle in the cloud when the LWP is above ~150 g/m^2. However, from Fig. 11 precipitation doesn't develop until the LWP is above ~200 g/m^2. The differences in the values of DWP below and above the cloud base for a similar amount of radiative flux divergence at the cloud top and total LWP suggests drizzle might be present within the cloud before it is detected below the cloud base. In addition, the amount of drizzle water within the cloud is greater than the amount below the cloud base for almost all values of radiative cooling and LWP.

5 Summary and conclusions

In this work Mie scattering by drizzle drops in the microwave spectrum is exploited to partition cloud and drizzle water path using data from active and passive sensors. Brightness temperature observations from a microwave radiometer, profiles of lidar attenuated backscatter and profiles of the first three moments of the radar Doppler spectra serve as an input to the retrieval algorithm. These data together with a radiative transfer code that includes Mie scattering calculations are used to derive parameters of drizzle DSD below the cloud base, total column LWP, and cloud and drizzle water path above the cloud base in marine boundary layer stratocumulus clouds. Due to the lack of coincident observations of in-cloud DWP via aircraft measurements, the retrieved cloud and drizzle water path above the cloud base during one day are qualitatively compared with the radar Doppler spectra between cloud base and cloud top. The analysis suggests that the optimal estimation algorithm utilizes the information provided by the radar and ceilometer on the drizzle below the cloud base to adjust the cloud water path and in-cloud drizzle water path to achieve convergence. The converged solution is broadly consistent with the partition between cloud and in-cloud drizzle water path extracted from the radar Doppler spectra.

The retrieval algorithm is applied to 20 days of precipitating stratocumulus cloud conditions at the ARM ENA site. Quantitative analysis of the cloud and drizzle water path during 20 days of precipitating events at the ENA site shows differences between closed and open cell scenarios. In the closed cell systems, only a small fraction (~20%) of the available drizzle in the cloud falls below the cloud base as compared to the open cell (~40%). Precipitation is associated with strong radiative cooling at the cloud top (less than -100 W/m^2) and higher liquid water path (higher than 200 g/m^2). However, drizzle in the cloud begins to exist at weak radiative cooling (divergence is greater than -80 W/m^2) and liquid water path higher than ~150 g/m^2. The amount of available drizzle that falls below the cloud base is higher (30-50 %) in open cell systems than in closed cell systems and is related to the average drizzle drop size. The average total drizzle water path in open cell drizzle shafts was fairly high, in all cases analyzed here it was higher than ~30 g/m^2 accounting for at least 20% of the total liquid water path retrieved by the radiometer. As the algorithm didn't converge during the highest precipitating intervals of the open cell drizzle shafts it is reasonable to conclude that the estimates provided here are in certain cases an underestimation. Additionally, smaller drizzle drops in the cloud are undetected because their scattering effect is negligible in the microwave leading to a possible underestimation of the in-cloud DWP even in closed cell systems.

The technique presented here can be readily applied to derive profiles of drizzle properties below the cloud base, cloud water path, drizzle water path above the cloud base, and total liquid water path under the following conditions, (i) the radar and ceilometer are not severely attenuated by precipitation, and are able to adequately detect the cloud base and cloud top, (ii) the radiometer measurements are not affected by precipitation on the radome, (iii) the drizzle droplet diameter is large enough to be detected by the 90 GHz channel and (iv) the cloud can be considered near-adiabatic to assume a priori cloud water content. Only single-layer stratocumulus clouds (closed cell) and precipitating stratocumulus clouds with non-precipitating shallow cumulus below (open cell) were analysed in this work. However, the technique should be applicable to different atmospheric conditions having observations from aircraft or satellite platforms because the primary limitation in this work is water accumulation on the ground-based radiometer radome.

Our results primarily highlight the need to account for scattering by drizzle drops while retrieving the column amount of liquid water (LWP) from the brightness temperatures observed by high frequency microwave radiometers. Precipitation is ubiquitous in marine stratocumulus clouds with much of it evaporating before reaching the surface (Zhou et al. 2015; Remillard et al. 2012; Serpetzoglou et al., 2008). The LWP can be inaccurate by traditional (satellite and ground-based) algorithms that neglect the scattering due to drizzle drops for clouds with LWP greater than 500 g/m^2. This can lead to inaccurate quantification of adiabaticity (e.g. Kim et al., 2003; Kim et al., 2008), precipitation susceptibility (e.g. Sorooshian et al. 2009), and aerosol-cloud interactions (e.g. McComiskey et al. 2009). LWP is also one of the primary metrics for evaluating single column model simulations and Large Eddy Simulation (LES) model in stratocumulus cloud conditions (e.g. Remillard et al. 2017; McGibbon and Bretherton, 2017). The ARM program has had a strong impact on furthering our understanding of aerosol-cloud-precipitation interactions (Feingold and McComiskey, 2016) and on cloud modeling at various scales (Kruger et al. 2016; Randall et al. 2016). Although preliminary, our analyses have impact on the conclusions of some of the previous studies. Objective quantification of the overestimation of the LWP by the traditional algorithms is a warranted and will be topic of our further study.

5 Author contribution

M.C. prepared the manuscript with contributions from all authors. V.G. preprocessed, cleaned and calibrated the radar and ceilometer data. M.C. performed the active and passive retrievals.

M.M. contributed to the development and compilation of PAMTRA and provided support to the use of the PAMTRA radiative transfer model.

5 Acknowledgements

VG was supported by the U.S. Department of Energy's (DOE) Atmospheric System Research (ASR), an Office of Science, Office of Biological and Environmental Research (BER) program, under Contract DE-AC02-06CH11357 awarded to Argonne National Laboratory. MC is supported by the U.S. Department of Energy, Office of Science, Office of Biological and Environmental Research, Atmospheric Radiation Measurement Infrastructure, under contract # DE-AC02-06CH11357. The ground-based data used in this study were obtained from the Atmospheric Radiation Measurement (ARM) user facility, a U.S. Department of Energy (DOE) Office of Science, user facility managed by the Office of Biological and Environmental Research.

References

Acquistapace, C., Löhnert, U., Maahn, M., Kollias, P.: A New Criterion to Improve Operational Drizzle Detection with Ground-Based Remote Sensing, J. Atmos. Ocean. Tech., 36, 781–801, doi: 10.1175/JTECH-D-18-0158.1, 2019.

Ahlgrimm, M., Forbes, R.: Improving the Representation of Low Clouds and Drizzle in the ECMWF Model Based on ARM Observations from the Azores, Month. Weath. Rev., 142, 668-685, DOI: 10.1175/MWR-D-13-00153.1, 2014.

Bosisio A., V., Fionda, E., Ciotti, P., Martellucci, P.: A sky status indicator to detect rain-affected atmospheric thermal emissions observed at ground, IEEE Trans. Geosci. Remote Sens., 51, 9, 4643–4649, 2013.

Cadeddu, M. P., Marchand, R., Orlandi, E., Turner, D. D., and Mech, M.: Microwave Passive Ground-Based Retrievals of Cloud and Rain Liquid Water Path in Drizzling Clouds: Challenges and Possibilities, IEEE Trans. Geosci. Remote. Sens., 55, 11, 6468–6481, 2017.

Cadeddu M. P., Turner, D. D., Liljegren, J. C.: A neural network for real-time retrievals of PWV and LWP from arctic millimeter-wave ground-based observations, IEEE Trans. Geosci. Remote Sens., 47, 7, 1887–1900, 2009.

Clothiaux, E. E., Ackerman, T.P., Mace, G. G., Moran, K. P., Marchand, R. T., Miller, M. A., and Martner, B. E.: Objective Determination of Cloud Heights and Radar Reflectivities Using a Combination of Active Remote Sensors at the ARM CART Sites, J. Appl. Meteor., 39, 645–665, DOI:10.1175/1520-0450(2000)039<0645:ODOCHA>2.0.CO;2, 2000.

Clough, S. A., Shephard, M. W., Mlawer, E. J., Delamere, J. S., Iacono, M. J., Cady-Pereira, K., Boukabara, S., Brown, P.D.: Atmospheric radiative transfer modeling: a summary of the AER codes, *J. Quant. Spectrosc. Radiat. Transf.*, 91, 233–244, 2005.

Evans K. F. and Stephens, G. L.: Microwave radiative transfer through clouds composed of realistically shaped ice crystals. Part II: Remote sensing of ice clouds, J. Atmos. Sci., 52, 2058–2072, 1995.

Feingold, G. and McComiskey, A.: ARM's Aerosol–Cloud–Precipitation Research (Aerosol Indirect Effects). Meteorological Monographs, 57, 22.1–22.15, doi:10.1175/AMSMONOGRAPHS-D-15-0022.1, 2016.

Fielding M. D., Chiu, J. C., Hogan, R. J., Feingold, G., Eloranta, E., O'Connor, E. J., and Cadeddu, M. P.: Joint retrievals of cloud and drizzle in marine boundary layer clouds using ground-based radar, lidar and zenith radiances, Atmos. Meas. Tech., 8, 2663–2683, doi: 10.5194/amt-8-2663-2015, 2015.

Frisch, A. S., Fairall, C. W. and Snider, J. B.: Measurement of Stratus Cloud and Drizzle Parameters in ASTEX with a K_{α}-Band Doppler Radar and a Microwave Radiometer, J. Atmos. Sci., 52, 16, 2788–2799, doi: 10.1175/15200469(1995)052<2788:MOSCAD>2.0.CO;2, 1995.

Frisch, S., Shupe, M., Djalalova, I., Feingold, G., Poellot, M.: The retrieval of stratus cloud droplet effective radius with cloud radars, J. Atmos. Ocean. Tech., 19, 6, 835–842, 2002.

Ghate, V. P., Cadeddu, M. P.: Drizzle and Turbulence Below Closed Cellular Marine Stratocumulus Clouds, J. Geophys. Res. Atmos., 124, 5724–5737, doi: 10.1029/2018JD030141, 2019.

Gossard, E. E., Strauch, R. G., Rogers, R. R.: Evolution of dropsize distribution in liquid precipitation observed by ground-based doppler radar, J. Atmos. Oceanic Tech., 7, 815–828, doi:10.1175/1520-0426(1990)007<0815: EODDIL>2.0.CO;2, 1990.

Han, Y. and Westwater, E. R.: Analysis and Improvement of Tipping Calibration for Ground-Based Microwave Radiometers, IEEE Trans. Geosci. Remote Sens., 38, 3, 1260–1276, 2000.

Hildebrand P.H., Sekhon, R. S.: Objective determination of the noise level in Doppler Spectra, J. Appl. Meteor. 13, 808–811, 1974.

Iacono, M. J., Mlawer, E. J., Clough, S. A., and Morcrette, J.-J.: Impact of an improved longwave radiation model, RRTM on the energy budget and thermodynamic properties of the NCAR Community Climate Model, CCM3, J. Geophys. Res., 105, 14873–14890, doi:10.1029/2000JD900091, 2000.

Jacob, M., Ament, F., Gutleben, M., Konow, H., Mech, M., Wirth, M., and Crewell, S.: Investigating the liquid water path over the tropical Atlantic with synergistic airborne measurements, Atmos. Meas. Tech., 12, 3237–3254, doi:10.5194/amt-12-3237-2019, 2019.

Kim, B.-G., Schwartz, S. E., Miller, M. A., and Min, Q.: Effective radius of cloud droplets by ground-based remote sensing: Relationship to aerosol, J. Geophys. Res., 108, D23, 4740, doi:10.1029/2003JD003721, 2003.

Kim, B.-G., Miller, M. A., Schwartz, S. E., Liu, Y., and Min, Q.: The role of adiabaticity in the aerosol first indirect effect, J. Geophys. Res., 113, D05210, doi:10.1029/2007JD008961, 2008.

Kollias, P., Rémillard. J., Luke, E., Szyrmer, W.: Cloud radar Doppler spectra in drizzling stratiform clouds: 1. Forward modeling and remote sensing applications, J. Geophys. Res., 116, D13201, doi:10.1029/2010JD015237, 2011a.

Kollias, P., Szyrmer, W., Rémillard, J., and Luke, E.: Cloud radar Doppler spectra in drizzling stratiform clouds: 2. Observations and microphysical modeling of drizzle evolution, J. Geophys. Res., 116, D13203, doi:10.1029/2010JD015238, 2011b.

Kotthaus, S., O'Connor, E., Münkel, C., Charlton-Perez, C., Haeffelin, M., Gabey, A. M., and Grimmond, C. S. B.: Recommendations for processing atmospheric attenuated backscatter profiles from Vaisala CL31 ceilometers, Atmos. Meas. Tech., 9, 3769–3791, 2016.

Krueger, S. K., Morrison, H., and Fridlind, A. M.: Cloud-Resolving Modeling: ARM and the GCSS Story, AMS Meteorological Monographs, 57, 25.1–25.16, 10.1175/AMSMONOGRAPHS-D-15-0047.1, 2016.

Lebsock, M. D., L'Ecuyer, T. S., and Stephens, G. L.: Detecting the Ratio of Rain and Cloud Water in Low-Latitude Shallow Marine Clouds, J. Appl. Meteor. Clim., 50 (2), 419–432, 2011.

Luke, E. and Kollias, P.: Separating Cloud and Drizzle Radar Moments during Precipitation Onset Using Doppler Spectra, J. Atmos. Oceanic Tech., 30, 1656–1671, doi: 10.1175/JTECH-D-11-00195.1, 2013.

Löhnert, U. and Crewell, S.: Accuracy of cloud liquid water path from ground-based microwave radiometry 1. Dependency on cloud model statistics, Radio Sci., 38, 8041–8051, doi:10.1029/2002RS002654, 2003.

McComiskey, A., Feingold, G., Frisch, A. S., Turner, D. D., Miller, M. A., Chiu, J. C., Min, Q., and Ogren, J. A: An assessment of aerosol-cloud interactions in marine stratus clouds based on surface remote sensing, J. Geophys. Res., 114, D09203, doi:10.1029/2008JD011006, 2009.

McGibbon, J. and Bretheron C. S.: Skill of ship-following large-eddy simulations in reproducing MAGIC observations across the northeast Pacific stratocumulus to cumulus transition, J. Adv. Model. Earth Syst., 9, 810–831, doi:10.1002/2017MS000924, 2017.

Mech, M., Maahn, M., Kneifel, S., Davide, O., Crewell, S., and Kollias P.: Passive and Active Microwave Transfer (PAMTRA), 9th Workshop of the International Precipitation Working Group, Seoul, South Korea, 5–9 November, P2.18, 2018.

O'Connor, E. J., Hogan, R. J. and Illingworth, A. J.: Retrieving Stratocumulus Drizzle Parameters Using Doppler Radar and Lidar. J. Appl. Meteor., 44, 14–27, 2005.

Painemal, D. and Zuidema, P.: Assessment of MODIS cloud effective radius and optical thickness retrievals over the Southeast Pacific with VOCALS_Rex in situ measurements, J. Geophys. Res., 116, D24206, doi: 10.1029/2011JD016155, 2011.

Randall, D. A., Del Genio, A. D., Donner, L. J., Collins, W. D., and Klein, S. A.: The Impact of ARM on Climate Modeling. AMS Meteorological Monographs, 57, 26.1–26.16, doi:10.1175/AMSMONOGRAPHS-D-15-0050.1, 2016.

Rémillard, J., Kollias, P., Luke, E., and Wood, R.: Marine Boundary Layer Cloud Observations in the Azores, J. Climate, 25, 7381–7398, doi:10.1175/JCLI-D-11-00610.1, 2012.

Rémillard, J., Fridlind, A. M., Ackerman, A. S., Tselioudis, G., Kollias, P., Mechem, D. B., Chandler, H. E., Luke, E., Wood, R., Witte, M. K., and Ayers, J. K.: Use of cloud radar Doppler spectra to evaluate stratocumulus drizzle size distributions in large-eddy simulations with size-resolved microphysics. *J. Appl. Meteorol. Climatol.*, 56, 12, 3263–3283, doi:10.1175/JAMC-D-17-0100.1, 2017.

Serpetzoglou, E., Albrecht, B. A., Kollias, P., and Fairall, C. W.: Boundary Layer, Cloud, and Drizzle Variability in the Southeast Pacific Stratocumulus Regime, J. Climate, 21, 6191–6214, doi:10.1175/2008JCLI2186.1, 2008.

Sorooshian, A., Feingold, G., Lebsock, M. D., Jiang, H., and Stephens G. L.: On the precipitation susceptibility of clouds to aerosol perturbations, Geophys. Res. Lett., 36, L13803, doi:10.1029/2009GL038993, 2009.

Turner, D. D., Clough, S. A., Liljegren, J. C., Clothiaux, E. E., Cady-Pereira, K., and Gaustad, K.L.: Retrieving liquid water path and precipitable water vapor from Atmospheric Radiation Measurement (ARM) microwave radiometers, IEEE Trans. Geosci. Remote Sens., 45, 3680–3690, doi:10.1109/TGRS.2007.903703, 2007.

Wall, C., Marchand, R., Zhao, W., Cadeddu, M. P.: An Assessment of rain "contamination" in ARM two-channel microwave radiometer measurements, ASR PI meeting, Tysons, VA, 13–17 March, 2017.

Wang, H., Feingold, G., Modeling Mesoscale Cellular Structures and Drizzle in Marine Stratocumulus. Part I: Impact of Drizzle on the Formation and Evolution of Open Cells, J. Atmos. Sci., 66, 3237-3256, 2009, DOI: 10.1175/2009JAS3022.1, 2009.

Wood, R.: Drizzle in Stratiform Boundary Layer Clouds. Part I: Vertical and Horizontal Structure, J. Atmos. Sci., 62, 3011–3033, 2005.

Wood, R., Comstock, K. K., Bretherton, C. S., Cornish, C., Tomlinson, J., Collins, D. R., and Fairall, C.: Open cellular structure in marine stratocumulus sheets, J. Geophys. Res., 113, D12207, doi:10.1029/2007JD009371, 2008.

Wood, R.: Stratocumulus Clouds, Mon. Weather. Rev., 40, 2373–2423, doi: 10.1175/MWR-D-11-00121.1, 2012.

Wood, R., Wyant, M., Bretherton, C. S., Rémillard, J., Kollias, P., Fletcher, J., Stemmler, J., De Szoeke, S., Yuter, S., Miller, M., Mechem, D., Tselioudis, G., Chiu, J. C., Mann, J. A. L., O'Connor, E. J., Hogan, R. J., Dong, X., Miller, M., Ghate, V., Jefferson, A., Min, Q., Minnis, P., Palikonda, R., Albrecht, B., Luke, E., Hannay, C., and Lin, Y.: Clouds, aerosols, and precipitation in the marine boundary layer. An ARM Mobile Facility Deployment, Bull. Amer. Meteor. Soc., 96, 419–440, 2015.

Yamaguchi, T., Feingold, G., Kazil, J.: Stratocumulus to Cumulus Transition by Drizzle, Journal of Advances in Modeling Earth Systems, 9, 2333–2349, doi: 10.1002/2017MS001104, 2017.

Zheng, X., Klein, S. A., Ma, H.-Y., Caldwell, P., Larson, V.E., Gettelman, A., and Bogenschutz, P.: A cloudy planetary boundary layer oscillation arising from the coupling of turbulence with precipitation in climate simulations. J. Adv. Model. Earth Syst., 9, 1973–1993, doi:10.1002/2017MS000993, 2017.

Zhou, X., Kollias, P., and Lewis, E. R.: Clouds, Precipitation, and Marine Boundary Layer Structure during the MAGIC Field Campaign, J. Climate, 28, 2420–2442, doi:10.1175/JCLI-D-14-00320.1, 2015.

Zuidema, P., Westwater, E. R., Fairall, C., Hazen, D.: Ship-based liquid water path estimates in marine stratocumulus, J. Geophys. Res., 110, D20206, doi: 10.1029/2005JD005833, 2005.

Table 1: The passive module of the retrieval algorithm. Mean values and standard deviations of a priori; retrieved quantities for all the cases where the retrieval converged are shown in red.

Step	**Variable**	**Initial Estimation**	
First guess water vapor	PWV [kg/m^2]	Statistical retrieval (*) 1.63±0.35; 1.59±0.36	
First guess total LWP	LWP_t [g/m^2]	Statistical retrieval (*) 114.1±136.7; 92.9±103.5	
		Below-cloud base	**In-cloud**
Average drizzle effective radius	D0d [μm]	Active retrieval 159.3±103.5	Constant=D0mix at cloud base 61.2±48.5
Cloud effective radius	D0c [μm]		Assumed = 20
First guess drizzle LWC	DWC	Active retrieval	Constant = LWCmix at cloud base (**)
First guess drizzle LWP	DWP [g/m^2]	Integrated from DWC_{bc} 6.4±12.7	Integrated from DWC_{ac} (**) 13.9±33.4; 10.4±24.9
First guess cloud LWP	CWP [g/m^2]		CWP=LWPt-DWP_{ac} (**) 100.3±114.8; 82.6±88.9
First guess cloud LWC	CWC		Assumed adiabatic (**)
First guess cloud to total LWP ratio	C_f	C_f=CWP/LWPt (*) 0.86±0.12; 0.92±0.15	

(*) Retrieved with passive module

(**) Adjusted during the retrieval to be consistent with integrated amounts

Table 2: Cloud, drizzle, and total LWP, for open cell cases (units are g/m^2).

Date	# shafts (min)	Total LWP	Below Cloud DWP (fraction of total DWP)	Above Cloud DWP** (fraction of total DWP)	DWP	CWP
20151207	8 (199)	303.51	24.98 (.38)	41.72 (.62)	66.70	236.81
20151230	4 (143)	172.94	15.09 (.43)	20.31 (.57)	35.40	159.66
20160113	10 (286)	214.49	15.66 (.40)	23.07 (.60)	38.72	176.66
20160329	9 (274)	152.87	12.02 (.42)	16.46 (.58)	28.48	143.75
20160411	11 (285)	135.51	15.39 (.58)	11.05 (.42)	26.44	122.54
20160508	8 (311)	182.07	13.20 (.42)	18.22 (.58)	31.41	151.39
20160509	9 (237)	128.20	10.74 (.39)	16.89 (.61)	27.63	117.87
20161022	12 (274)	212.72	20.38 (.55)	16.56 (.45)	36.95	185.96
20161104	5 (158)	174.66	10.37 (.31)	22.69 (.69)	33.05	141.61
20161121	13 (434)	233.95	15.92 (.27)	43.05 (.73)	58.97	174.98
All	89 (2651)	194.68±158.27	15.84±19.02 (.40)	23.3±26.96 (.60)	39.15±35.11	162.11±131.98

Table 3: Above and below cloud drizzle diameter, cloud top temperature, optical depth and geometrical thickness for open cell cases.

Date	# shafts (min)	Above cloud base drizzle diameter (μm)	Below cloud base drizzle diameter (μm)	CTT (K)	Optical depth	Geometrical thickness (km)
20151207	8 (199)	153.76	331.19	269.9	35.5	1.1
20151230	4 (143)	123.28	214.08	280.4	23.9	0.73
20160113	10 (286)	106.63	182.42	279.5	26.5	0.70
20160329	9 (274)	90.69	261.65	279.8	21.6	1.06
20160411	11 (285)	125.39	270.97	270.9	18.4	0.97
20160508	8 (311)	105.91	229.35	274.5	22.7	1.0
20160509	9 (237)	90.23	189.39	275.8	17.7	0.99
20161022	12 (274)	110.88	232.68	279.7	27.9	1.00
20161104	5 (158)	85.47	137.35	280.9	21.2	0.59
20161121	13 (434)	92.17	189.67	279.9	26.2	1.02
All	89 (2651)	107.68±55.41	225.99±118.23	277.46±5.74	24.32±19.80	0.93±0.44

Table 4: Cloud, drizzle, and total LWP, for closed cell cases (units are g/m^2).

Date	#shafts (min)	Total LWP	Below Cloud DWP (fraction of total DWP)	Above Cloud DWP (fraction of total DWP)	DWP	CWP
20151019	3 (97)	210.8	2.25 (.17)	12.14 (.83)	14.57	196.26
20160227	5 (417)	138.06	4.47 (.20)	18.76 (.80)	23.40	114.66
20160303	3 (97)	183.34	0.49 (.15)	3.04 (.85)	3.54	179.80
20160304	3 (212)	215.57	1.20 (.14)	8.27 (.87)	9.49	206.08
20160409	10 (492)	158.87	3.68 (.25)	11.52 (.75)	15.27	143.60
20160628	9 (550)	123.49	3.46 (.20)	15.42 (.80)	19.25	104.25
20161015	5 (439)	143.53	6.73 (.23)	23.93 (.77)	30.72	112.81
20161031	13 (575)	158.20	3.53 (.24)	11.02 (.76)	14.57	143.63
20161116	8 (368)	212.43	8.96 (.16)	29.09 (.84)	34.46	177.98
20161117	8 (436)	129.96	9.92 (.29)	23.87 (.71)	33.53	96.42
All	65 (3603)	159.95±56.20	4.97±5.32 (.22)	16.31±14.38 (.78)	20.91±18.21	139.05±49.88

Table 5: Above and below cloud drizzle diameter, cloud top temperature, optical depth and geometrical thickness for closed cell cases.

Date	#shafts (min)	Above cloud base drizzle diameter (μm)	Below cloud base drizzle diameter (μm)	CTT (K)	Optical depth	Geometrical thickness (km)
20151019	3 (97)	44.88	133.52	286.7	29.4	0.71
20160227	5 (417)	53.45	145.43	280.9	17.2	0.57
20160303	3 (97)	37.77	138.29	285.4	26.9	0.48
20160304	3 (212)	42.79	170.49	282.5	30.9	0.65
20160409	10 (492)	50.02	142.41	283.7	21.5	0.70
20160628	9 (550)	49.56	180.67	288.1	15.6	0.30
20161015	5 (439)	61.30	146.47	279.1	16.9	0.66
20161031	13 (575)	46.29	131.38	281.4	21.5	0.91
20161116	8 (368)	57.49	158.56	285.8	26.7	0.43
20161117	8 (436)	61.78	141.43	283.3	14.5	0.54
All	65 (3603)	51.46±14.90	147.77±43.68	283.74±3.19	20.85±7.48	0.61±0.26

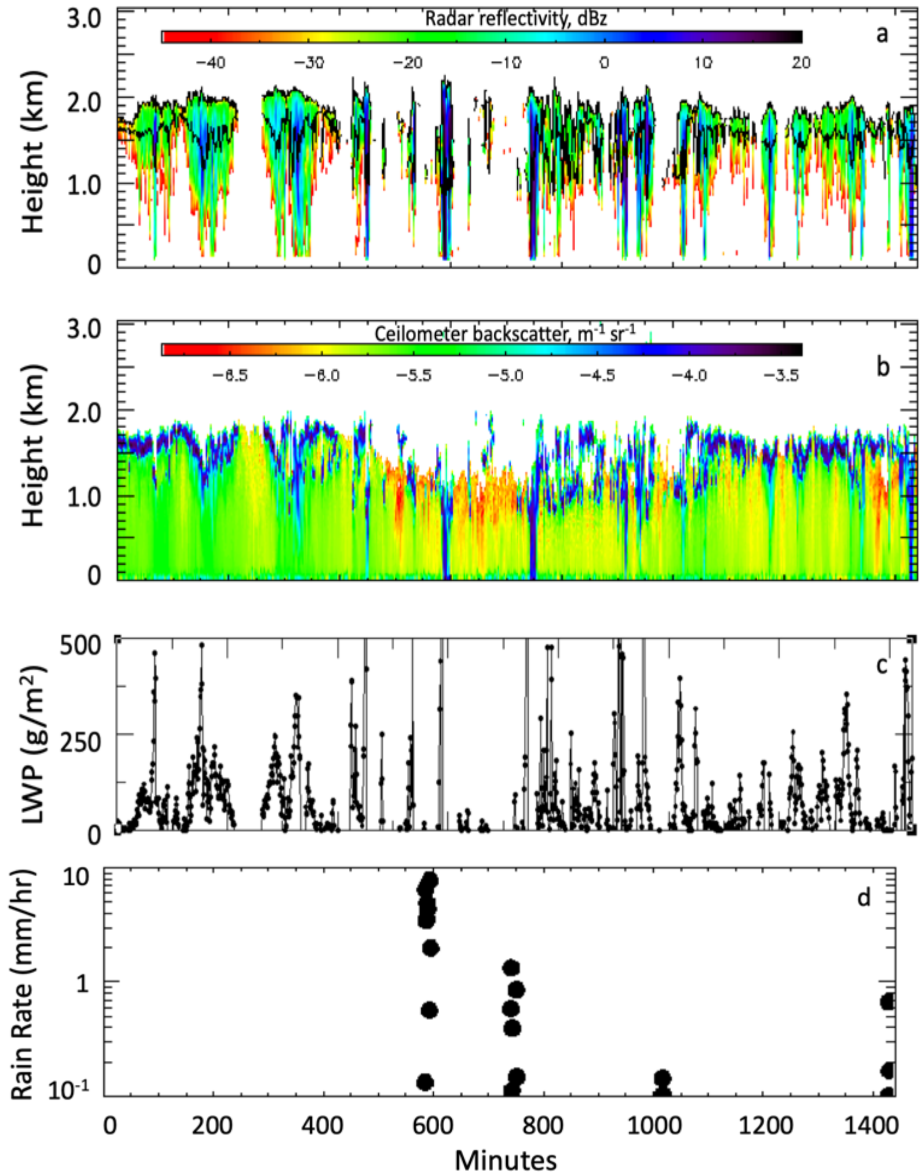

Figure 1: (a) Time-height profiles of KAZR reported reflectivity (shades) together with cloud boundaries from KAZR (cloud top) and ceilometer (cloud base) in black, (b) time-height profiles of ceilometer attenuated backscatter (shades), (c) time-series of microwave radiometer reported LWP from MWRRETv2 (Turner, 2007), and (d) Rain rate at the surface from video-disdrometer (log scale). The data were collected on 21 November 2016. Data in a and b are 1-minute averaged, data in c are smoothed with a 5-min running average.

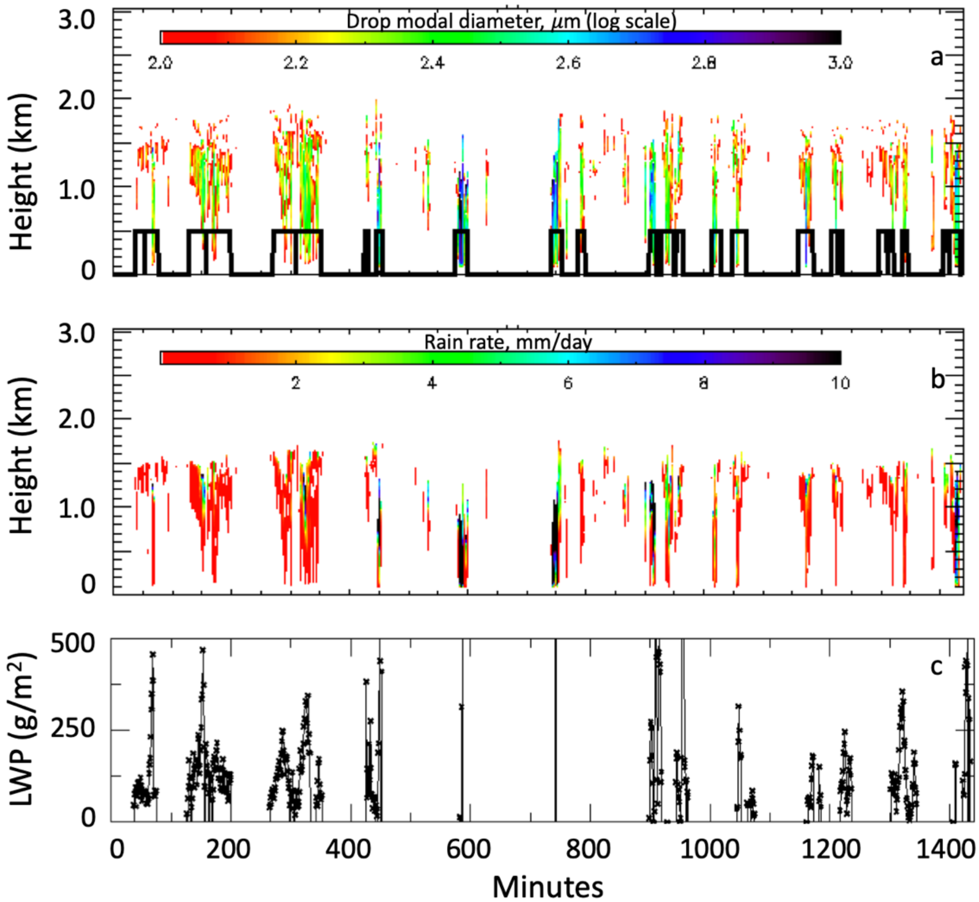

Figure 2: (a) Time-height profiles of retrieved drizzle drop modal diameter below cloud (shades) and identified drizzle shafts (black line) (b) time-height profiles of rain rate and (c) time-series of retrieved LWP during precipitating shafts using PAMTRA. The data were collected on 21 November 2016. Data in (a) and (b) are 1-minute averaged, data in c are smoothed with a 5-min running average. The drizzle mode diameter in (a) is shown in log scale between 100 and 1000 μm.

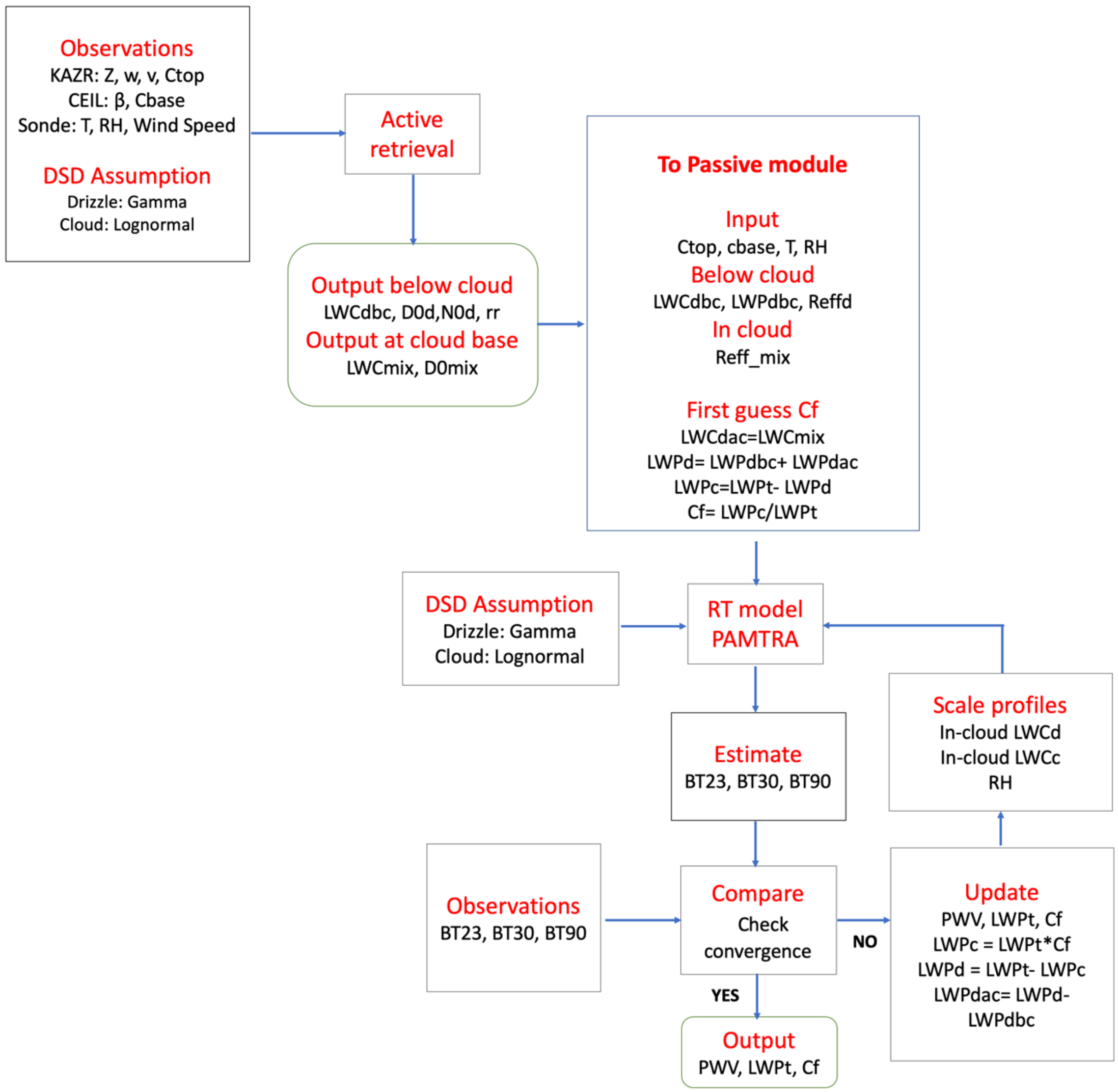

Figure 3: Flow chart of the active and passive modules.

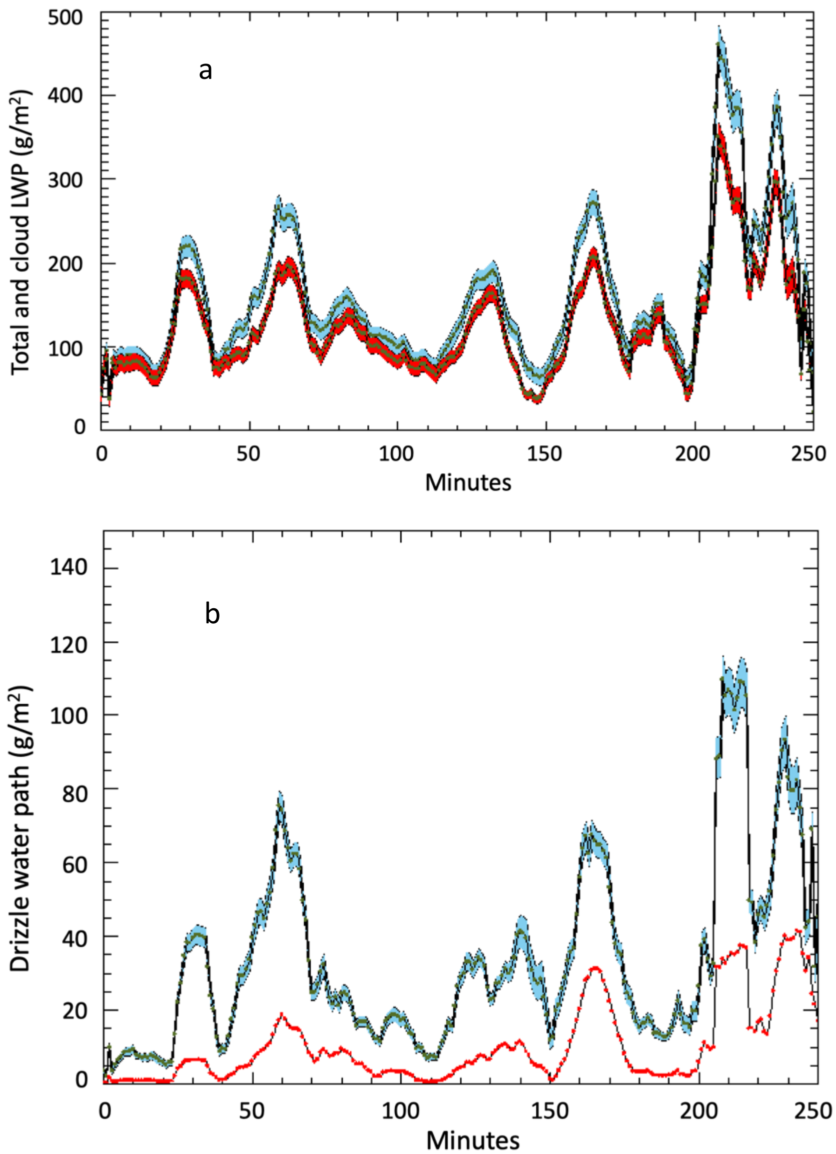

Figure 4: (a) Total (blue) and cloud (red) LWP. (b) Total drizzle water path (blue) and below-cloud drizzle water path (red) between 00 and 04 UTC on 21 November 2016. The data are smoothed with a 10-min boxcar average for better readability. Shaded regions represent the 1-sigma uncertainty provided by the optimal estimation algorithm.

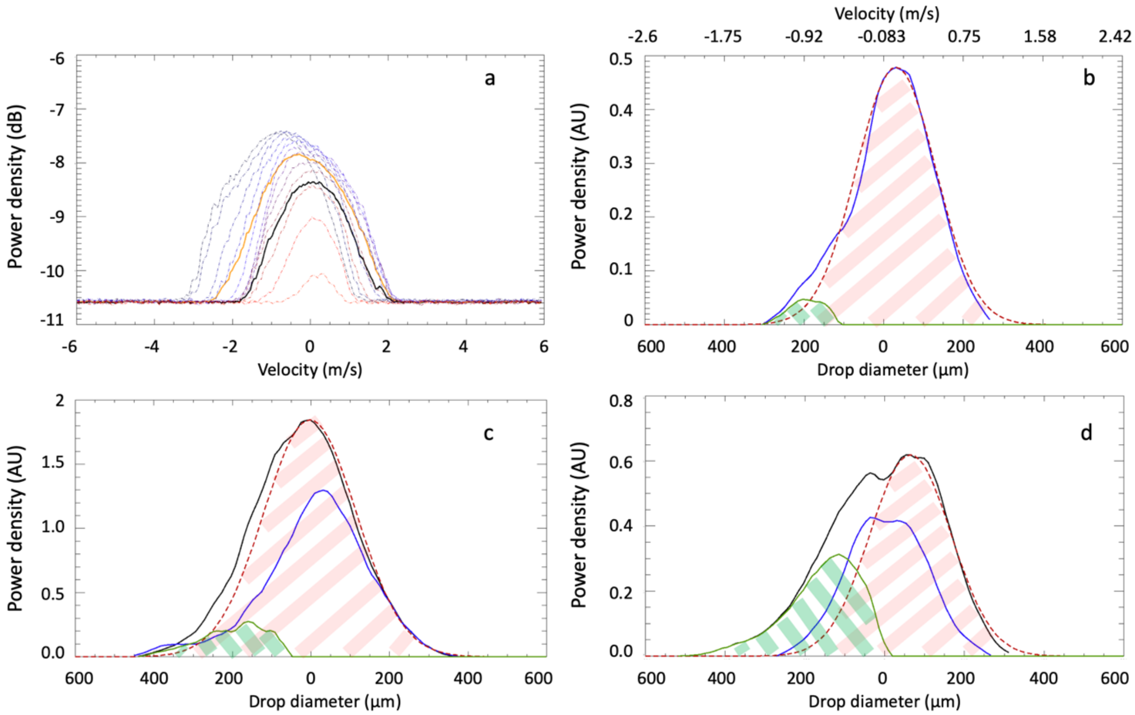

Figure 5: (a) Radar Doppler spectra between cloud base and cloud top at 04:30 UTC on November 21, 2016. (b–d) Doppler spectra averaged between cloud base and cloud top (black), averaged over cloud-only layers (blue), Gaussian fitted curve (red), drizzle component (green) at 04:29 (b), 04:35 (c), and 04:56 (d) UTC. The black line in (b) is entirely under the blue line. All Doppler spectra are minute averaged. On the top x-axis of the left panel the velocity corresponding to the calculated diameter is shown. Negative velocities refer to downward motion. The drop diameter in the x-axis was derived using the size-velocity relation in Gossard et al. (1990).

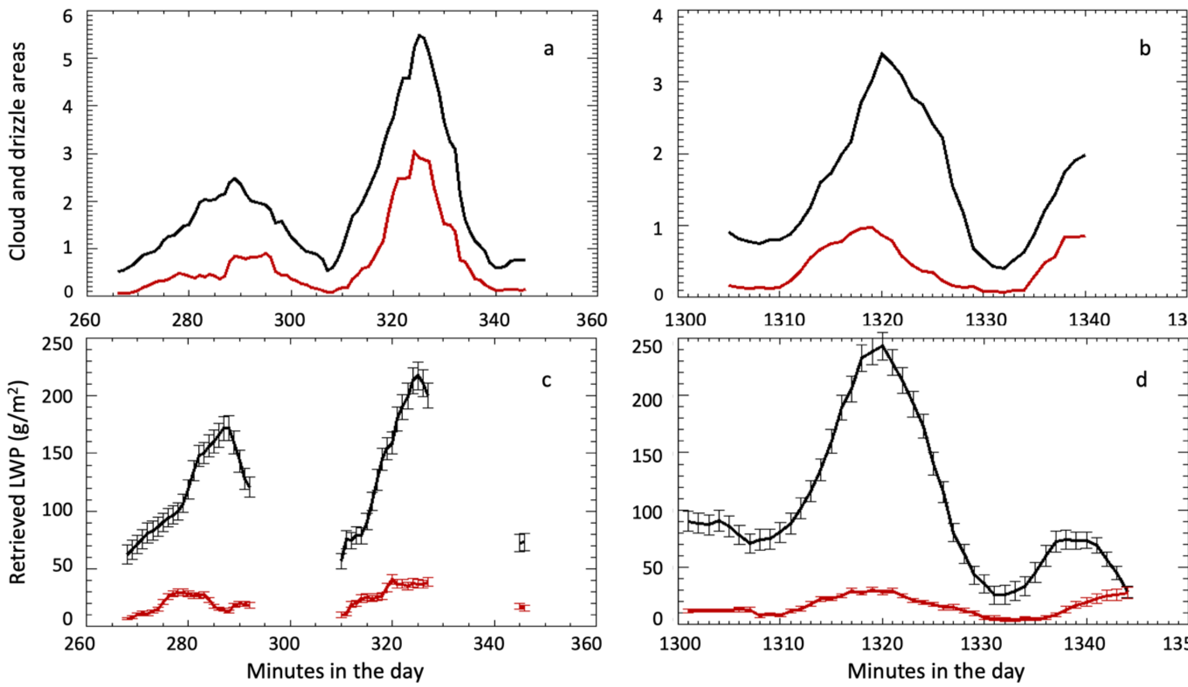

Figure 6: Cloud (black) and drizzle (red) areas derived from Doppler spectra during two precipitating shafts at 4:22–5:50 UTC (a) and 21:41–22:24 UTC (b) on November 21, 2016. In the bottom panels corresponding cloud LWP (black), and in-cloud drizzle water path (red) estimated by the passive module are shown for the same drizzle shafts (c, d).

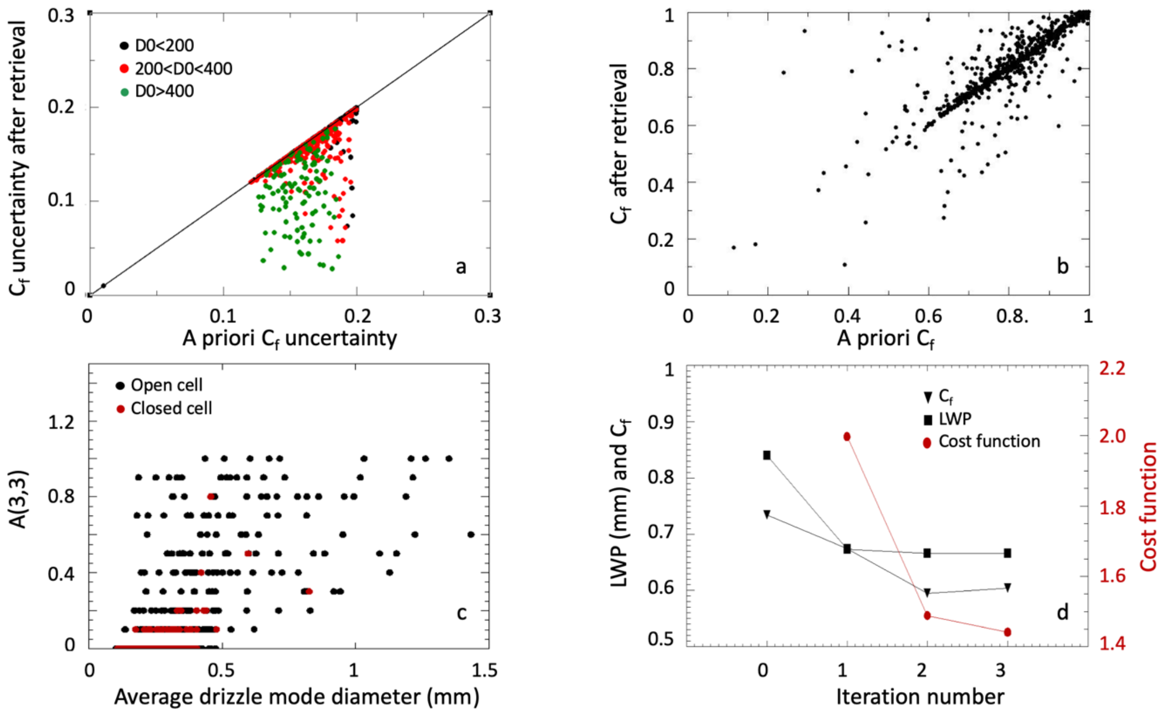

Figure 7: Scatter plot between (a) a priori C_f uncertainty and C_f uncertainty after the retrieval; (b) A priori C_f and C_f estimated with the retrieval for samples with LWP greater than 150 g/m^2; (c) A(3,3) dependence on the drizzle average mode diameter; (d) Changes in total LWP (black squares), C_f (black triangles), and cost function (red circles) during the convergence process for one retrieval point.

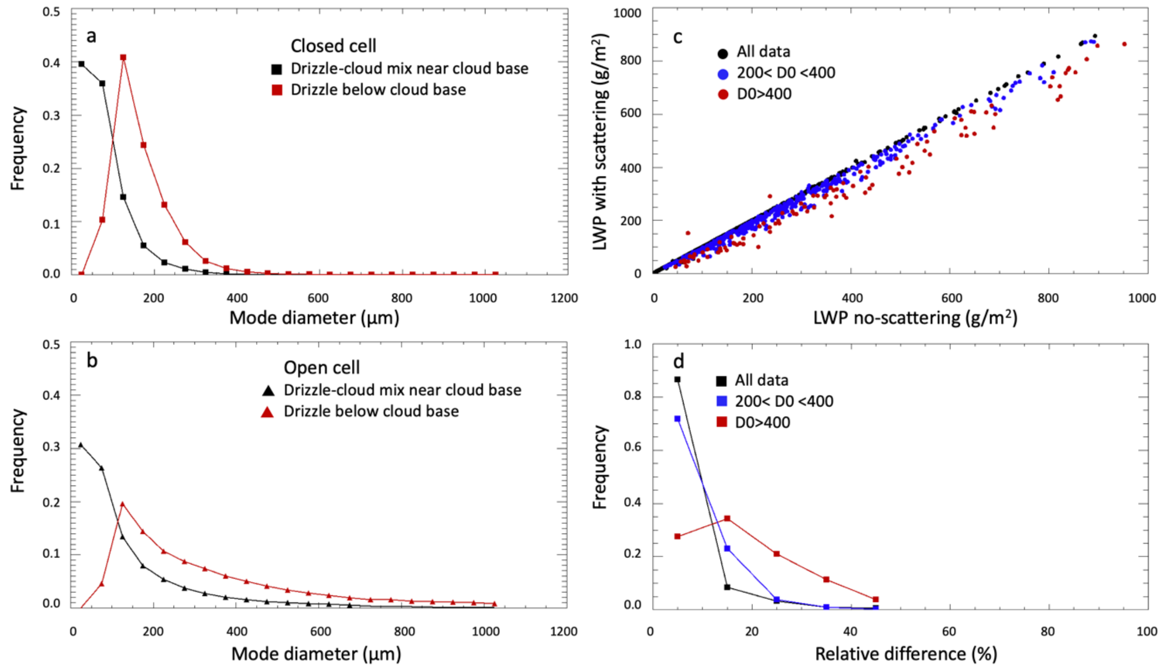

Figure 8: Distributions of retrieved mode diameter for closed cell (a) and open cell (b) cases. Red symbols represent drizzle below cloud base, black symbols represent cloud-drizzle mix immediately above the cloud base. (c): Scatterplot of total LWP retrieved with and without scattering effects. (d): Relative difference between total LWP retrieved without and with scattering segregated by below-cloud drizzle mode diameter.

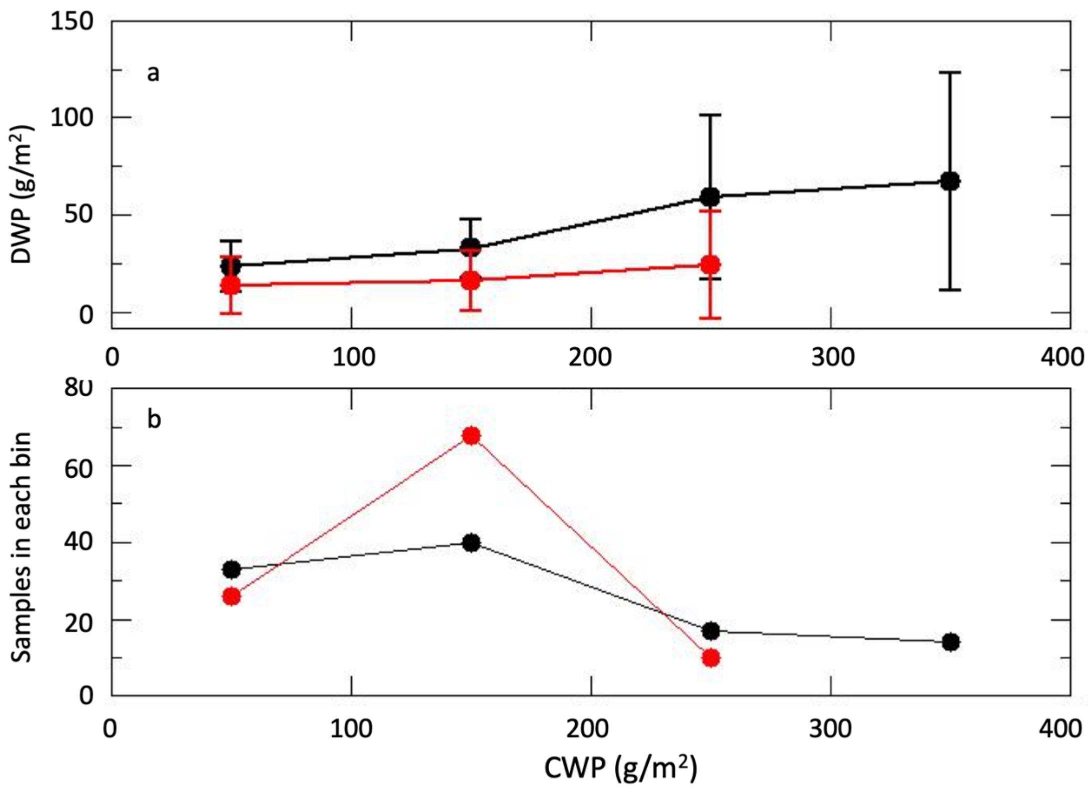

Figure 9: (a) Mean and standard deviation of cloud and drizzle water path for open cell (black) and closed cell (red) drizzle shafts. (b) Number of samples in each bin for open cell (black) and closed cell (red) drizzle shafts.

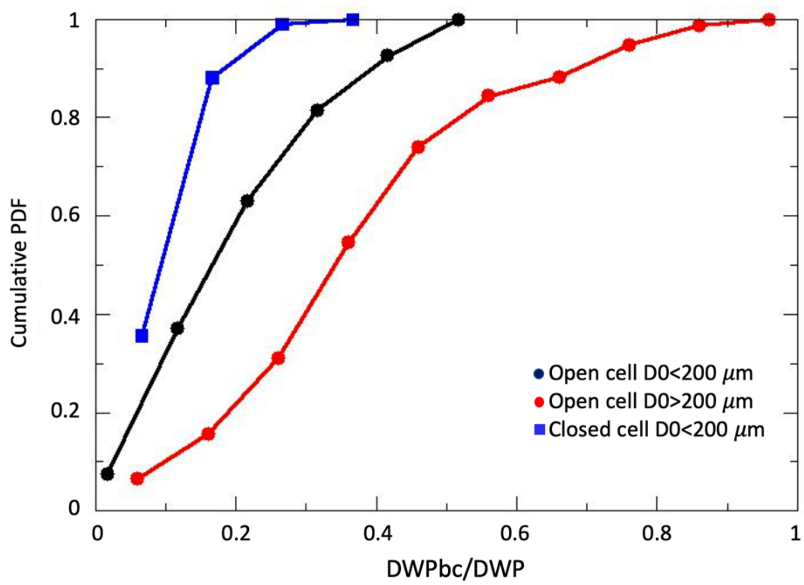

Figure 10: (a) Cumulative distribution of below-cloud to total drizzle water path for open and closed cell cases segregated by drizzle modal diameter (D0) at the cloud base.

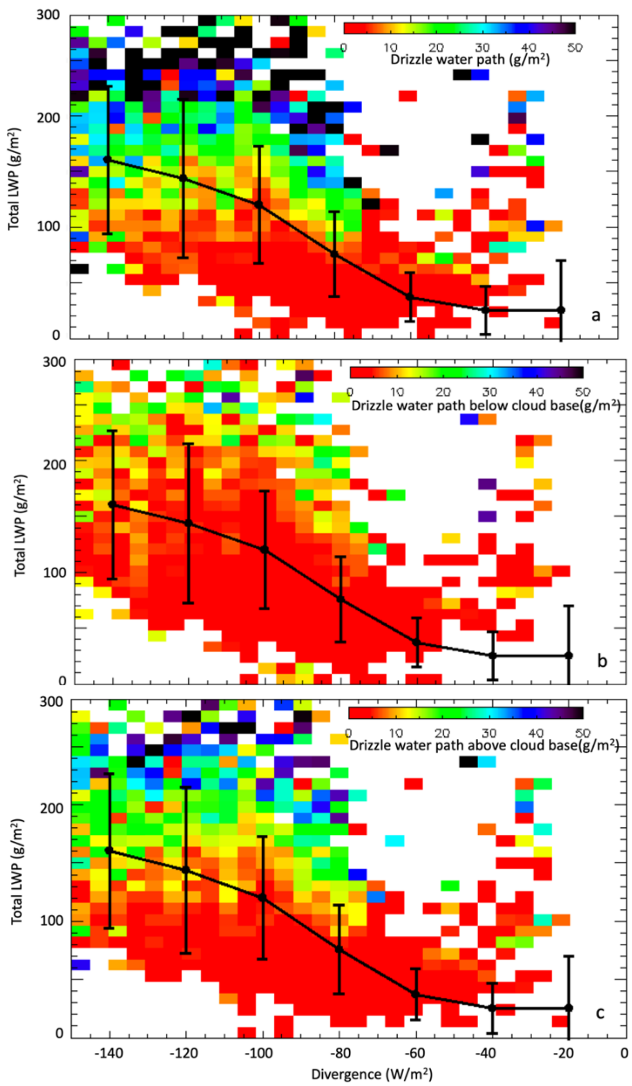

Figure 11: (a) Total, (b) below cloud base, and (c) in-cloud drizzle water path binned by radiative divergence and total liquid water path. The black circles connected by a solid line represent the total LWP binned by flux divergence and the vertical bars represent the standard deviation of the data in each bin.